Supporting Information

Multifunctional "Add-on" Module Enabled NIR-II-guided Synergistic Photothermal and Chemotherapy of Drug-resistant Lung Cancer

Yu Li [a§], Qiang Zhu [a§], Pei He [a§], Tingjuan Wu [a], Zhen Ouyang [c], Lijun Zhu [a], Fang Wang [a], Xin Zhou [a,b], Zhong-Xing Jiang [a,b]*, and Shizhen Chen [a,b]*

[a]*Innovation Academy for Precision Measurement Science and Technology, Chinese Academy of Sciences-Wuhan National Laboratory for Optoelectronics, Huazhong University of Science and Technology, Wuhan 430071, China*

[b]*University of Chinese Academy of Sciences, Beijing 100049, China*

[c]*School of Pharmaceutical Sciences, Wuhan University, Wuhan 430071, China*

*Email: zxjiang@apm.ac.cn, chenshizhen@apm.ac.cn

§*Y.L., Q.Z. and P.H. contributed equally to this work*

Table of Contents

1. General Information

Materials

Unless otherwise noted, solvents and reagents were purchased from commercial suppliers and used as received. Phospholipid S95 was purchased from Lipoid GmbH (Germany). Pluronic F68 (average MW = 8350 Da.) was obtained from Adamas (Shanghai, China). Cy5-DSPE-PEG2000 was purchased from Yusi (Chongqing, China). The human lung adenocarcinoma cell line (A549) was purchased from Beyotime (Shanghai, China), Human normal lung epithelial cell line (BEAS-2B) was purchased from Wuhan Xavier Biotechnology Co., LTD. Human lung adenocarcinoma cell/DOX-resistant strain A549/DOX was purchased from Shanghai Fuyu Biotechnology Co., LTD. The cells were cultured in Dulbecco's Modified Eagle's Medium (DMEM) supplemented with 10% fetal bovine serum (FBS) and 1% penicillin-streptomycin. Cells were incubated at 37 ^{o}C in a humidified 5% CO_2 atmosphere. Cell Counting Kit-8 (CCK-8), DAPI, and Calcein/PI staining were purchased from Beyotime (Shanghai, China). RIPA lysis buffer were purchased from Boerfu (Wuhan, China). Anti-P-gp antibody was puchased from Proteintech (Wuhan, China).

Female BALB/c nude mice at the age of 5-6 weeks were purchased from Hubei BIONT Biological Technology Co., Ltd. (Hubei, China). All animal experiments strictly adhered to the Guideline for Animal Care and Use, Innovation Academy for Precision Measurement Science and Technology, Chinese Academy of Sciences.

Methods

^{1}H and ^{13}C NMR spectra were acquired on Bruker 500 MHz spectrometers. ^{1}H NMR spectra were referenced to tetramethylsilane (s, 0.00 ppm) using $CDCl_3$ as solvent. ^{13}C NMR spectra were referenced to solvent carbons (77.16 ppm for $CDCl_3$). The splitting patterns for ^{1}H NMR spectra were denoted as follows: s = singlet, d = doublet, t = triplet, q = quartet, dd = double doublet, m = multiplet. MALDI-TOF mass spectra were recorded on a Bruker Ultraflex III TOF/TOF spectrometer. Flash chromatography was performed on 200-300 mesh silica gel with ethyl acetate (EtOAc)/petroleum ether (PE, 60-90 ^{o}C) as eluent. The UV−Vis and fluorescence emission spectra were measured via a UV-2600 UV−Vis spectrophotometer (Shimadzu, Japan) and an F-4700 spectrofluoro-photometer (Hitachi, Japan), respectively. Absolute fluorescence quantum yields were measured using a steady-state photoluminescence spectrometer (Edinburgh, FLS1000). The average particle size and polydispersity index (PDI) of nanoemulsions were measured by dynamic light scattering (DLS) with Zetasizer of Malvern (Malvern, Nano ZS 90, UK). The morphology of the nanomulsion was observed using transmission electron microscopy (TEM, JEM-2100, JEOL). Confocal laser scanning microscope (CLSM) images were performed on a Nikon confocal laser scanning microscope. Small animal fluorescence imaging was carried out by the NIR-II fluorescence imaging system(NIROPTICS, China). Photothermal imaging was measured by a thermal imaging camera (Zhejiang Dali Technology, China).

2. Supplementary Figures and Tables

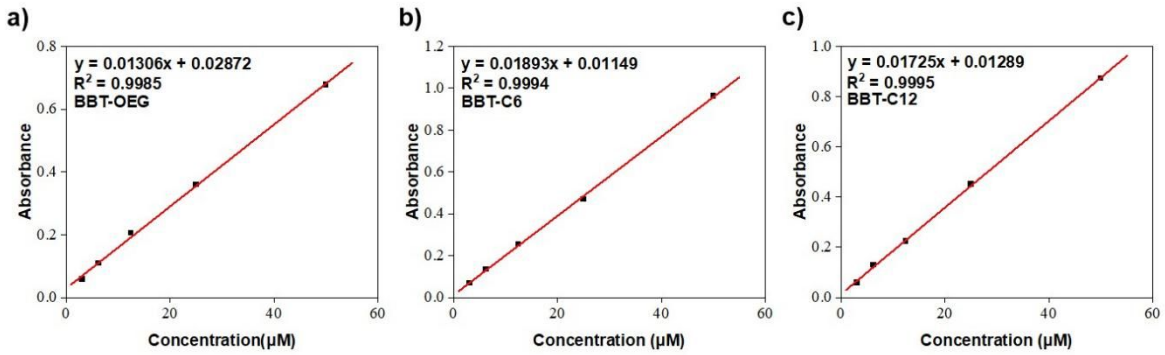

Figure S1. The calibration curves of **BBT-OEG** (a), **BBT-C6** (b), and **BBT-C12** (c) in *n*-octanol.

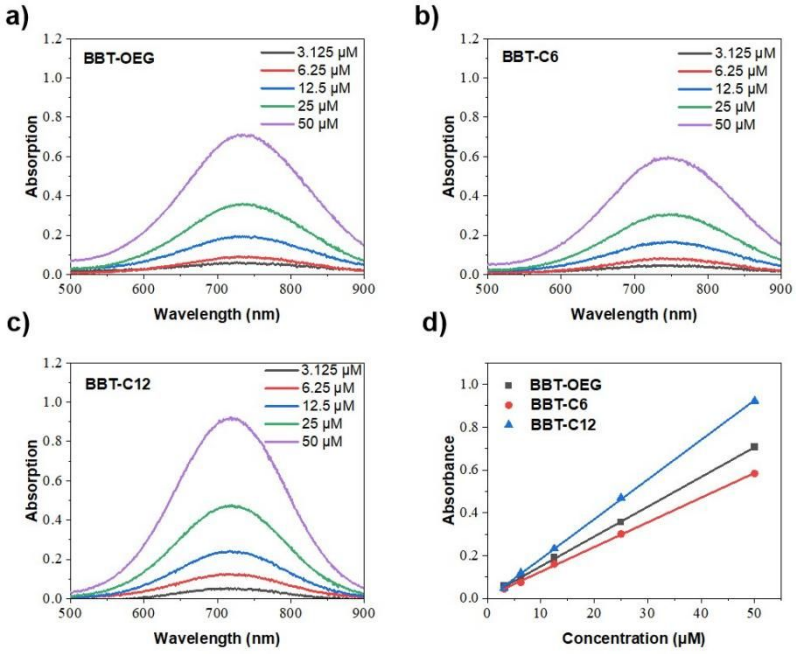

Figure S2. UV absorption spectra of **BBT-OEG** (a), **BBT-C6** (b), and **BBT-C12** (c) at the indicated concentrations. Linear fitting curves for concentration-dependent UV absorption (d).

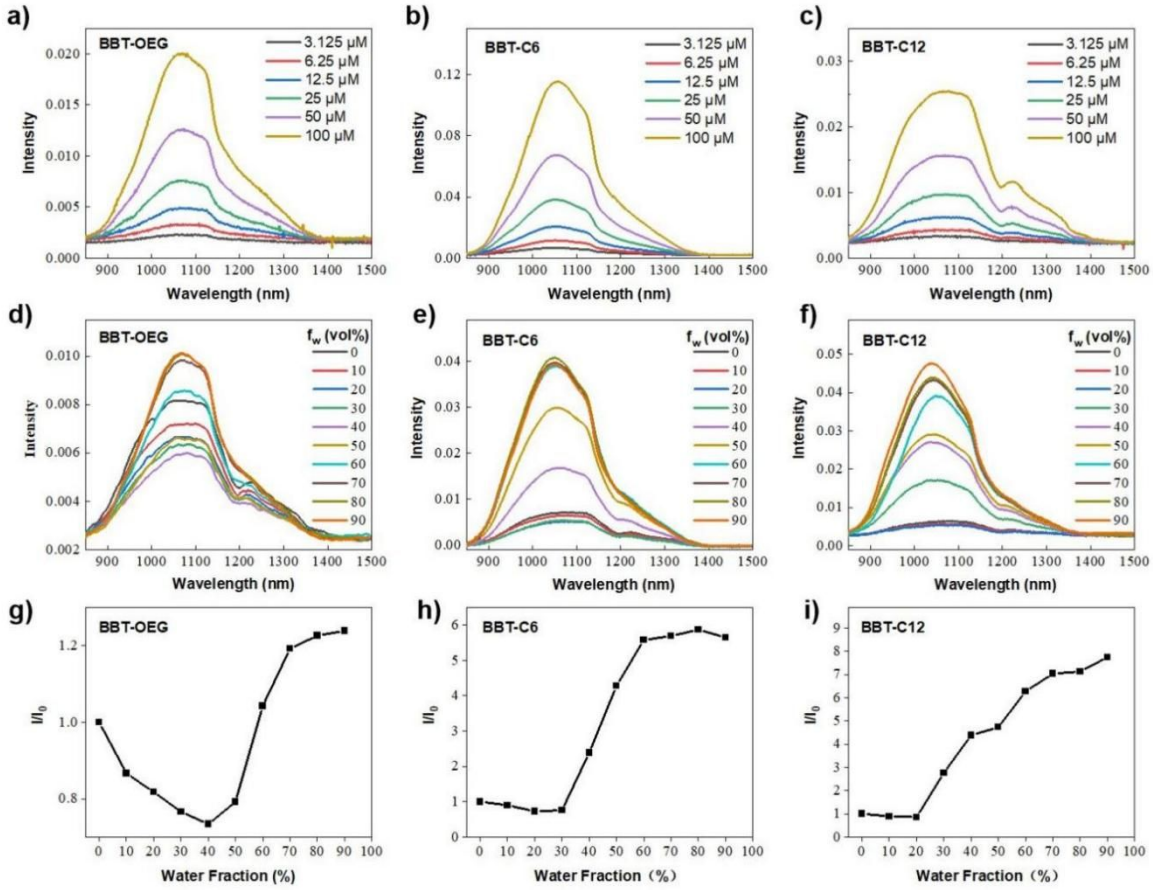

Figure S3. Fluorescence emission spectra of **BBT-OEG**, **BBT-C6**, and **BBT-C12** at different concentrations in water (for **BBT-OEG** and **BBT-C6**) or methanol (for **BBT-C12**) (a-c). Fluorescence emission spectra of **BBT-OEG**, **BBT-C6**, and **BBT-C12** in solutions of varying water content mixed with methanol (d-f). Quantitative fluorescence intensity plots (g-i). Excitation wavelength: 808 nm.

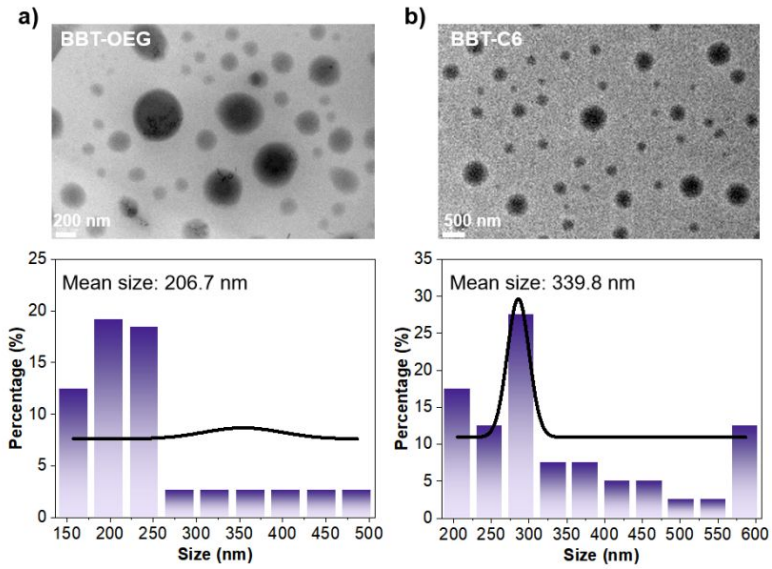

Figure S4. TEM images and size distribution of **BBT-OEG** (a, scale bar: 200 nm) and **BBT-C6** (b, scale bar: 500 nm).

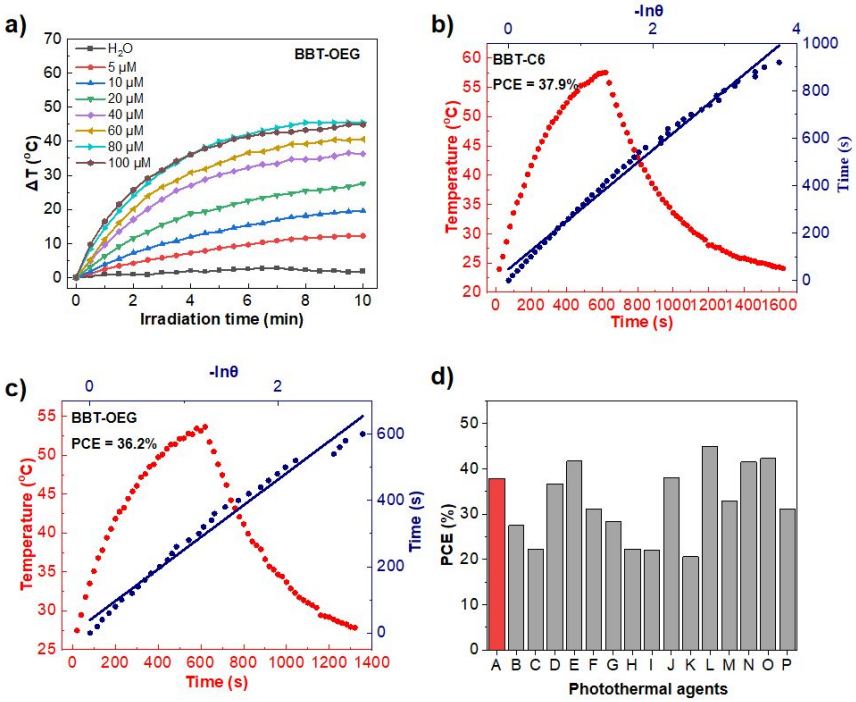

Figure S5. Temperature changes of **BBT-OEG** at a range of concentrations (a). The photothermic heating curves and photothermal conversion efficiency (PCE) calculation of a 30 μM of **BBT-C6** solution (b) and 30 μM of **BBT-OEG** solution (c). PCEs comparison of reported PTT agents with NIR-II fluorescence (under 808 nm laser irradiation): A) **BBT-C6**; B) **BPBBT**[1]; C) **SY1080**[2]; D) **PBPTV**[3]; E) **2TT-2BBTD**[4]; F) **NIRb10**[5]; G) **ZSY-TPE**[6]; H) **SYL**[7]; I) **TQTPA**[8]; J) **TTQ-TC-PFru**[9]; K) **H2a-4T**[10]; L) **SPN_{I-II}**[11]; M) **BBTD-TP**[12]; N) **DPP-OPIC**[13]; O) **PF**[14]; P) **P_3**[15] (d). 808 nm laser irradiation at 1.0 W/cm^2 was used in all cases.

Table S1 Compounds characterization data.

Compounds	MW	Log P	λ_{abs} (nm)	λ_{em} (nm)	ε	Φ (%)	CMC (μM)	η (%)
BBT-OEG	2967.4	-1.31	743	1074	14296	0.02	12	36.2
BBT-C6	3304.0	1.61	746	1056	11968	0.28	15.4	37.9
BBT- C12	3640.8	1.92	721	1041	18734	0.17	---	---

MW: molecular weight. Log P: n-octanol-water partition coefficients. λ_{abs}: near-infrared absorption. λ_{em}: second near-infrared fluorescence emission. ε: molar extinction coefficient, $L*mol^{-1}*cm^{-1}$. Φ: fluorescence quantum yield. CMC: critical micelle concentrations. η: photothermal conversion efficiency.

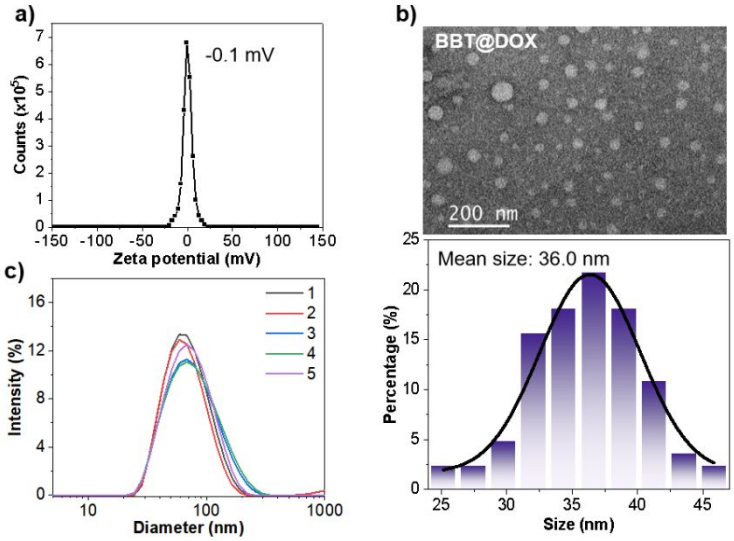

d)

Batches	Size (± SD, nm)	PDI (± SD)
1	64.4±0.7	0.197±0.026
2	67.3±0.8	0.241±0.002
3	69.9±0.6	0.233±0.008
4	68.5±2.0	0.212±0.003
5	67.0±0.5	0.225±0.002

Figure S6. Zeta potential of **BBT@DOX** (a). TEM images and size distribution of **BBT@DOX** (b, scale bar: 200 nm). DLS results of 5 batches of **BBT@DOX** (c, d).

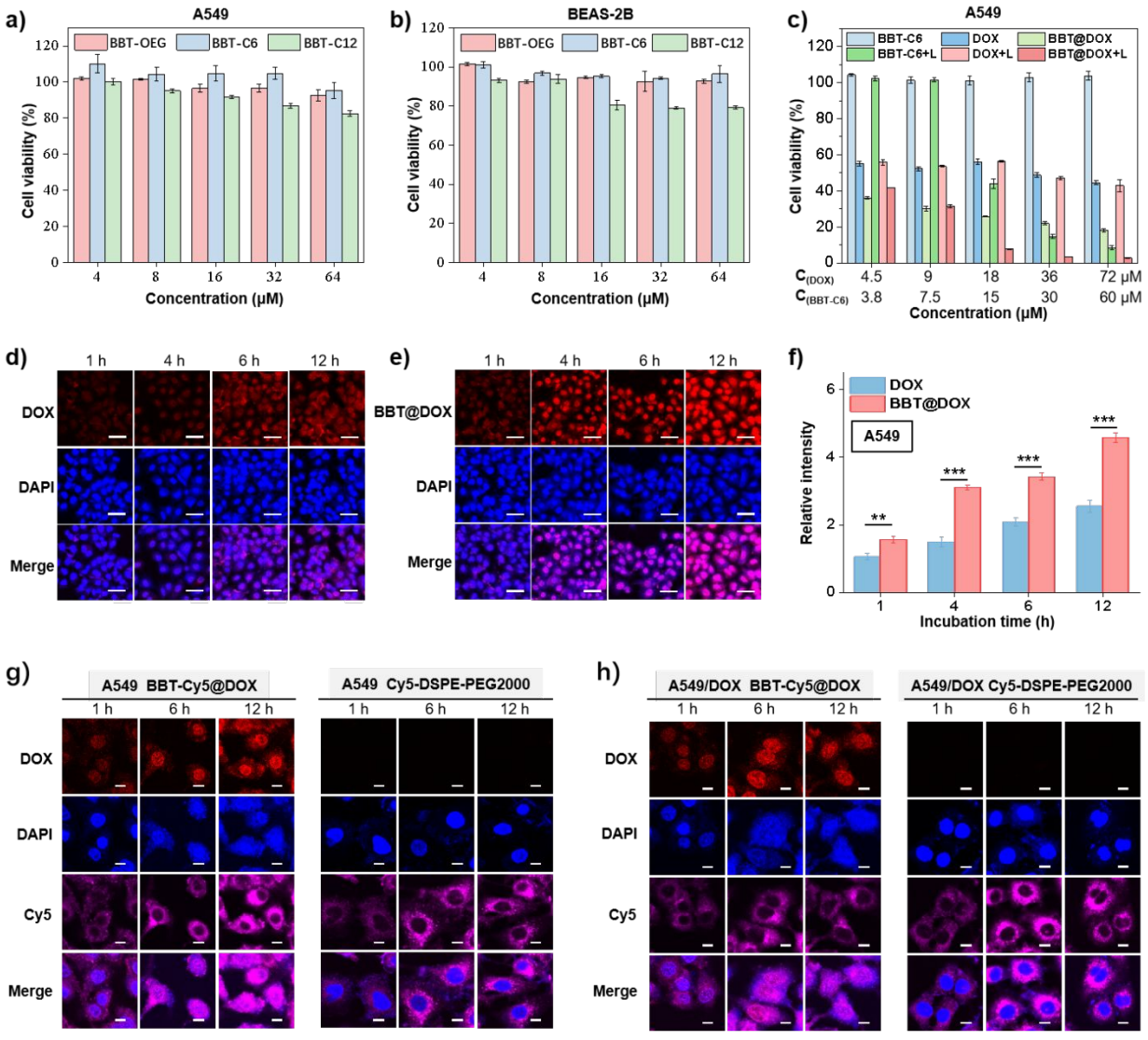

Figure S7. Biocompatibility assays of **BBT-OEG**, **BBT-C6**, and **BBT-C12** towards A549 cells (a) and BEAS-2B cells (b). Cell viability of A549 cells with different treatments (c). Data were expressed as means ± standard deviation (n = 3). Confocal microscope images of DOX- and BBT@DOX-treated A549 cells (d, e, Scale bar: 50 μm), and their quantitative analysis (f). Confocal microscope images of **BBT-Cy5@DOX**- and Cy5-DSPE-PEG-treated A549 cells (g, Scale bar: 10 μm) and A549/DOX cells (h, Scale bar: 10 μm).

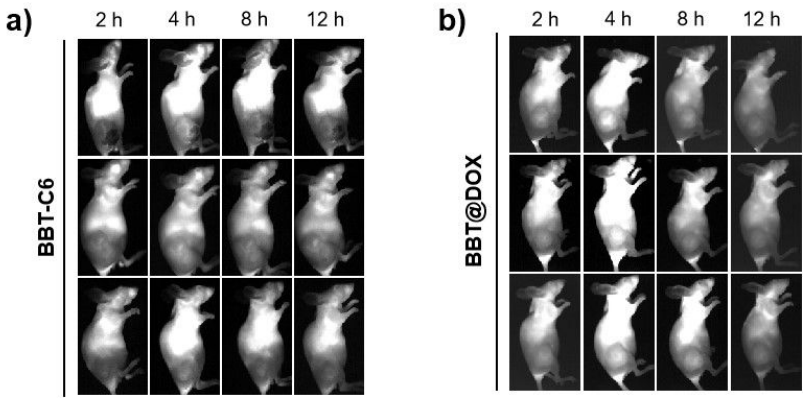

Figure S8. Whole-body NIR-II FL images of BALB/c nude mice bearing xenograft A549 lung tumors after i.v. injection of **BBT-C6** (a) and **BBT@DOX** (b). 1000 nm filters.

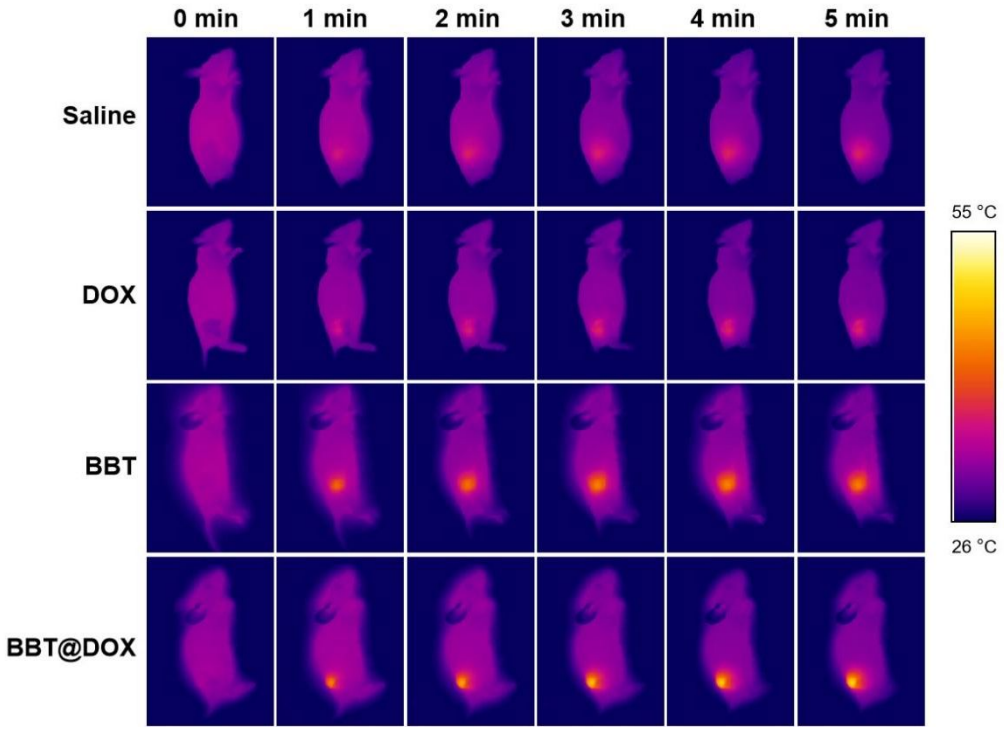

Figure S9. Real-time infrared thermal images of BALB/c nude mice bearing xenograft A549 lung tumors after the indicated i.v. injection. 808 nm laser irradiation at 0.8 W/cm^2 was used.

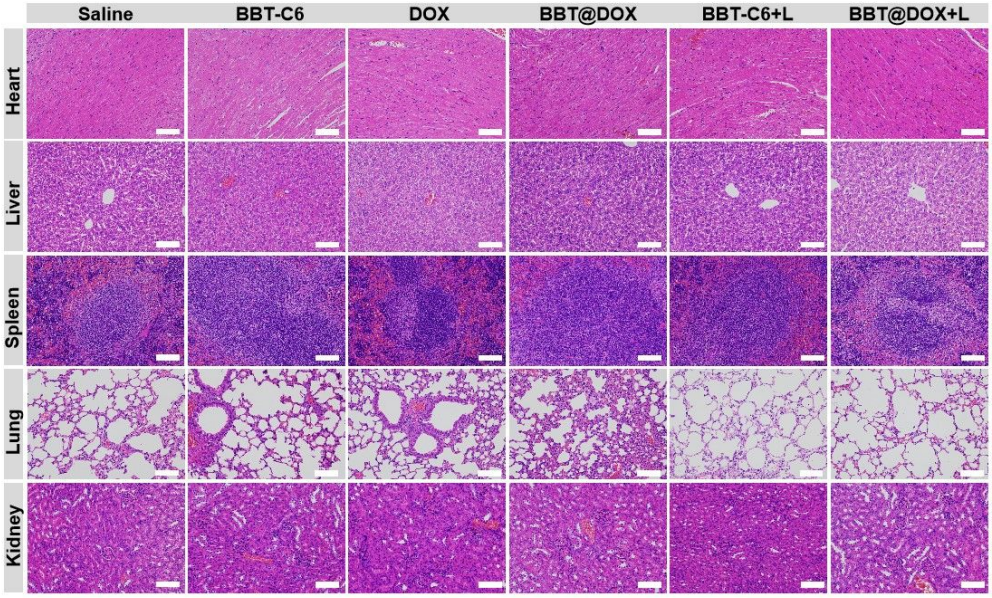

Figure S10. H&E staining of internal organs from the treatment groups (scale bar: 100 μm). Treatment was performed on BALB/c nude mice bearing xenograft A549 lung tumors.

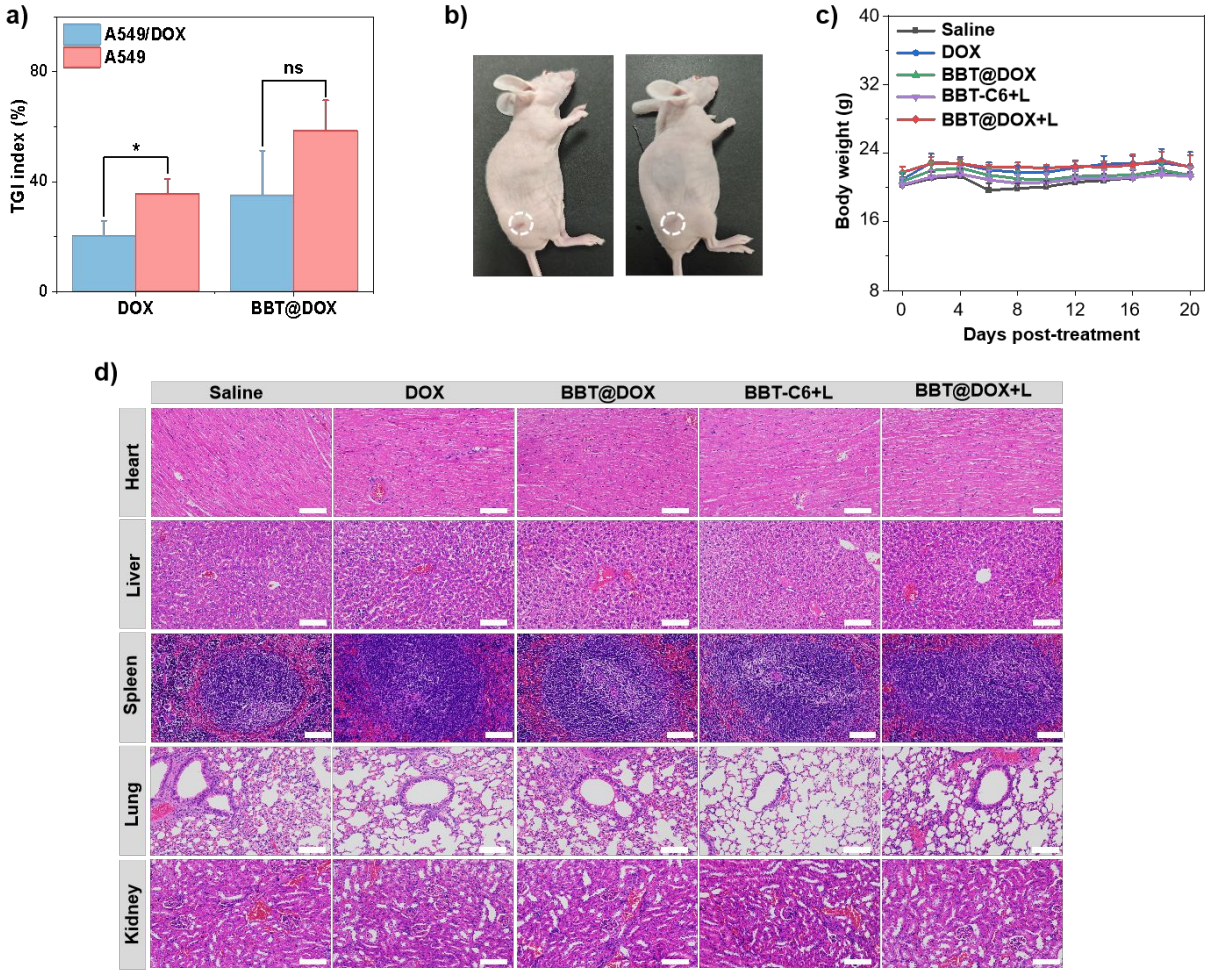

Figure S11. Significance analysis of the TGI indexes of DOX and BBT@DOX in treating both A549 tumors and

drug-resistant A549/DOX tumors (a). Photographs of representative mice from the **BBT@DOX**+laser group on day 20 (b). Body weight curves of the treatment groups (c). Treatment was performed on BALB/c nude mice bearing xenograft A549/DOX lung tumors (d) (scale bar: 100 μm). $n = 4$, the asterisks indicate the statistical significance, *ns*: not significant, $*p < 0.05$.

3. Synthesis and Characterization of **BBT-OEG**, **BBT-C6**, and **BBT-C12.**

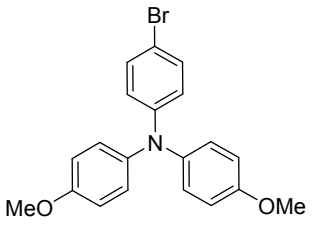

Compound 2: To a stirring solution of 4,4'-Dimethoxytriphenylamine (4.0 g, 13.1 mmol) in tetrahydrofuran (THF) (50 mL), a solution of NBS (2.6 g, 14.4 mmol, in THF) was slowly added at 0 ℃. The resulting mixture was stirred in the dark for 3 h. After thin layer chromatography (TLC) indicated complete consumption of 4,4'-Dimethoxytriphenylamine, the reaction mixture was quenched with water and concentrated under reduced pressure. The residue was dissolved in dichloromethane (DCM), and washed with saturated sodium thiosulfate and water (three times). The organic phase was dried over anhydrous sodium sulfate, filtered, and concentrated under reduced pressure. The crude product was purified by column chromatography on silica gel (petroleum ether/ethyl acetate (PE/EA) = 10/1) to obtain compound **2** as a white wax (4.9 g, 97% yield). ^{1}H NMR (500 MHz, Chloroform-*d*) δ 7.23 (d, *J* = 8.9 Hz, 2H), 7.03 (d, *J* = 9.0 Hz, 4H), 6.82 (d, *J* = 9.0 Hz, 4H), 6.79 (d, *J* = 8.9 Hz, 2H), 3.79 (s, 6H).

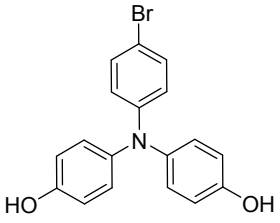

Compound 3: Under an atmosphere of nitrogen, compound **2** (4.7 g, 12.3 mmol) was dissolved in dry DCM (50 mL), and BBr_3 (18.4 g, 73.5 mmol) was slowly added to the solution. The resulting mixture was stirred at room temperature for 2 h in the dark. After TLC showed the completion of the reaction, the mixture was quenched with iced water. The organic phase was collected and concentrated under reduced pressure. The residue was purified by column chromatography on silica gel (PE/EA = 4/1) to obtain compound **3** as a white wax (3.3 g, 76% yield). ^{1}H NMR (500 MHz, Acetonitrile-d_3) δ 7.24 (d, *J* = 9.0 Hz, 2H), 7.04 – 6.93 (m, 6H), 6.78 (s, 4H), 6.69 (d, *J* = 9.0 Hz, 2H).

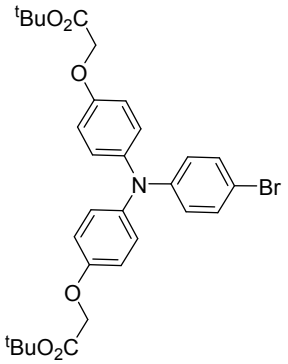

Compound 4a: Under an atmosphere of nitrogen, compound **3** (1.4 g, 3.8 mmol) and K_2CO_3 (3.2 g, 22.8 mmol) were dispersed in DMF and stirred at 80 ℃ for 30 minutes. Subsequently, *tert*-butyl bromoacetate (3.0 g, 15.4 mmol) was added, and the reaction was maintained at 80 ℃ for 16 h. Upon completion of the reaction as indicated by TLC, water was added to quench the reaction, and the product was extracted with EA. The organic phase was washed with brine three times, dried over anhydrous sodium sulfate, and concentrated under reduced pressure. The residue was purified by column chromatography on silica gel (PE:EA = 10:1) to obtain compound **4a** as a yellow liquid (1.9 g, 88% yield). ^{1}H NMR (500 MHz, Chloroform-*d*) δ 7.24 (d, *J* = 8.9 Hz, 2H), 6.99 (d, *J* = 8.9 Hz, 4H), 6.80 (d, *J* = 8.9 Hz, 6H), 4.48 (s, 4H), 1.49 (s, 18H). ^{13}C NMR (126 MHz, Chloroform-*d*) δ 168.1, 154.3, 147.7, 141.3, 131.8, 126.3, 122.7, 115.6, 113.0, 82.4, 66.1, 28.1. MS (MALDI-TOF) *m/z*: $[M+H_3O]^+$ calcd for $C_{30}H_{35}BrNO_6^+$ 584.165; found 584.898.

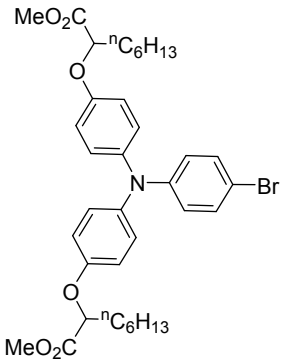

Compound 4b was synthesized using the same method as **4a** and was purified by silica gel column (light yellow liquid, 2.9 g, 92% yield). ^{1}H NMR (500 MHz, Chloroform-*d*) δ 7.22 (d, *J* = 8.8 Hz, 2H), 6.97 (d, *J* = 8.9 Hz, 4H), 6.81 – 6.75 (m, 6H), 4.55 (m, 2H), 3.75 (s, 6H), 1.97 – 1.86 (m, 4H), 1.59 – 1.43 (m, 4H), 1.38 – 1.28 (m, 12H), 0.88 (t, *J* = 6.8 Hz, 6H). ^{13}C NMR (126 MHz, Chloroform-*d*) δ 172.5, 154.3, 147.7, 141.3, 131.9, 126.4, 122.7, 116.1, 113.0, 77.0, 52.2, 33.0, 31.6, 28.9, 25.3, 22.6, 14.1. MS (MALDI-TOF) *m/z*: $[M-H]^-$ calcd for $C_{36}H_{45}BrNO_6^-$ 666.243; found 666.978.

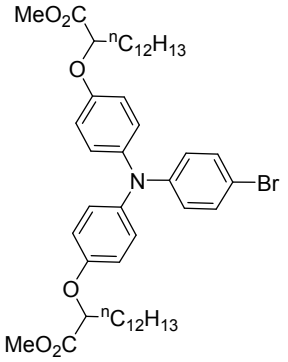

Compound 4c was synthesized using the same method as **4a** and was purified by silica gel column (yellow liquid, 4.0 g, 82% yield). ^{1}H NMR (500 MHz, Chloroform-*d*) δ 7.23 (d, *J* = 8.9 Hz, 2H), 6.97 (d, *J* = 8.9 Hz, 4H), 6.81 – 6.75 (m, 6H), 4.54 (m, 2H), 3.76 (s, 6H), 1.97 – 1.87 (m, 4H), 1.55 – 1.44 (m, 4H), 1.33 – 1.25 (m, 36H), 0.88 (t, *J* = 6.9 Hz, 6H). ^{13}C NMR (126 MHz, Chloroform-*d*) δ 172.5, 154.3, 147.6, 141.3, 131.8, 126.3, 122.7, 116.0, 113.0, 52.2, 32.9, 31.9, 29.7, 29.65, 29.63, 29.5, 29.40, 29.36, 29.2, 25.3, 22.7, 14.1. MS (MALDI-TOF) *m/z*: $[M+H_3O]^+$ calcd for $C_{48}H_{71}BrNO_6^+$ 836.447; found 837.075.

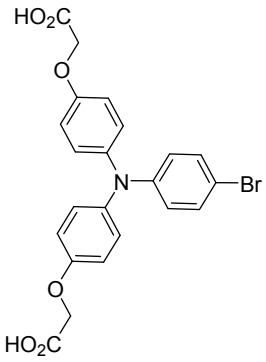

Compound 5a: Compound **4a** (1.9 g, 3.3 mmol) and anisole (0.5 g, 4.9 mmol) were dissolved in dry DCM (30 mL), and trifluoroacetic acid (7.4 g, 64.9 mmol) was added. Upon completion of the reaction as indicated by TLC, the solvent was removed under reduced pressure. The crude product was purified by recrystallization, yielding compound **5a** as a white solid (1.0 g, 62% yield), which could be used directly in the subsequent reaction without further purification.

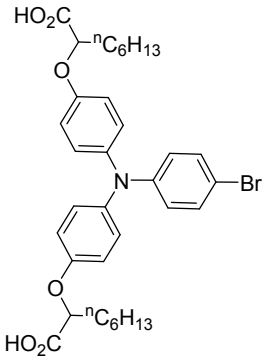

Compound 5b: Compound **4b** (3.2 g, 4.8 mmol) and NaOH (3.9 g, 97.5 mmol) were dissolved in a mixture of DCM : MeOH (200 mL, 9:1) and reacted at room temperature for 4 h. After TLC indicated the completion of the reaction, the solvent was removed under reduced pressure. The pH was adjusted to 3.0 by

acidification with dilute hydrochloric acid, and the organic phase was extracted by DCM. The combined organic phases were dried over anhydrous sodium sulfate, and filtered, yielding a light yellow liquid **5b** (3.1 g, 99% yield). The crude product could be used directly in the subsequent reaction without further purification.

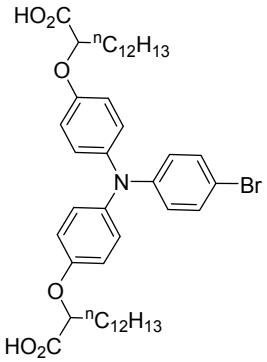

Compound 5c was synthesized using the same method as **5b** and obtained as a light yellow liquid (2.7 g, 98% yield).

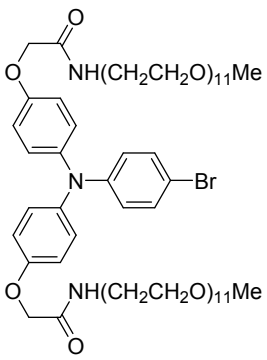

Compound 6a: Under an atmosphere of nitrogen, compound **5a** (1.0 g, 2.0 mmol), diisopropylcarbodiimide (DIC, 0.8 g, 6.0 mmol), and 1-hydroxybenzotriazole (HOBt, 0.8 g, 6.0 mmol) were dissolved in DMF (25 mL), and the mixture was stirred in a 45 ℃ for 30 min. A solution of amino-PEG_{11}-OMe[16] (3.1 g, 6.0 mmol) dissolved in DMF (25 mL) was then added to the reaction mixture and stirred at 45 ℃ for 12 h. Upon TLC indicating completion of the reaction, the mixture was washed with saturated $NaHCO_3$ solution and brine. The organic phase was collected, dried, filtered, and purified by flash chromatography on silica gel (DCM:MeOH = 20:1) to obtain **6a** as a light yellow liquid (2.1 g, 70% yield). ^{1}H NMR (500 MHz, Chloroform-*d*) δ 7.26 (d, *J* = 8.9 Hz, 2H), 7.05 (t, *J* = 5.6 Hz, 2H), 7.01 (d, *J* = 9.0 Hz, 4H), 6.84 – 6.79 (m, 6H), 4.45 (s, 4H), 3.66 – 3.60 (m, 80H), 3.56 – 3.52 (m, 8H), 3.37 (s, 6H). ^{13}C NMR (126 MHz, Chloroform-*d*) δ 168.2, 153.6, 147.4, 141.8, 132.0, 126.3, 123.0, 115.8, 113.5, 71.9, 70.6, 70.6, 70.5, 70.3, 69.8, 67.8, 59.0, 38.8. MS (MALDI-TOF) *m/z*: $[M+Na]^+$ calcd for $C_{68}H_{112}BrN_3NaO_{26}^+$ 1488.662; found 1489.028.

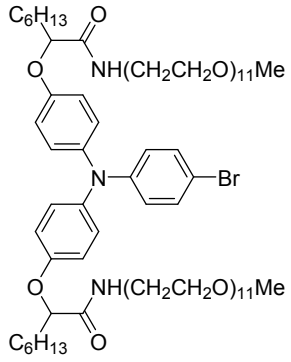

Compound 6b was synthesized using the same method as **6a** and obtained as a light yellow liquid (6.5 g, 83% yield). ^{1}H NMR (500 MHz, Chloroform-*d*) δ 7.21 (d, *J* = 8.5 Hz, 2H), 6.93 (d, *J* = 8.6 Hz, 4H), 6.81 (t, *J* = 5.6 Hz, 2H), 6.78 – 6.74 (m, 6H), 4.42 (m, 2H), 3.64 – 3.51 (m, 80H), 3.49 – 3.42 (m, 8H), 3.33 (s, 6H), 1.92 – 1.77 (m, 4H), 1.48 – 1.36 (m, 4H), 1.31 – 1.21 (m, 12H), 0.83 (t, *J* = 6.7 Hz, 6H). ^{13}C NMR (126 MHz, Chloroform-*d*) δ 171.7, 154.0, 147.4, 141.6, 131.9, 126.2, 122.9, 116.6, 113.3, 79.8, 71.9, 70.6, 70.6, 70.51, 70.48, 70.3, 69.8, 59.0, 38.7, 33.2, 31.6, 29.0, 25.0, 22.5, 14.1. MS (MALDI-TOF) *m/z*: $[M+Na]^+$ calcd for $C_{80}H_{136}BrN_3NaO_{26}^+$ 1656.849; found 1657.087.

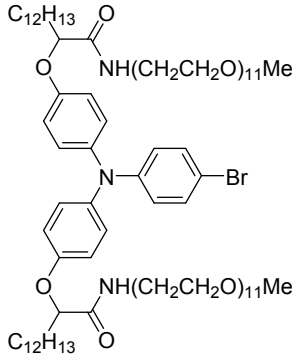

Compound 6c was synthesized using the same method as **6a** and obtained as a light yellow liquid (3.0 g, 87% yield). ^{1}H NMR (500 MHz, Chloroform-*d*) δ 7.25 (d, *J* = 9.0 Hz, 2H), 6.97 (d, *J* = 9.0 Hz, 4H), 6.84 (t, *J* = 5.7 Hz, 2H), 6.81 – 6.78 (m, 6H), 4.45 (m, 2H), 3.66 – 3.47 (m, 88H), 3.37 (s, 6H), 1.94 – 1.83 (m, 4H), 1.50 – 1.40 (m, 4H), 1.30 – 1.23 (m, 36H), 0.87 (t, *J* = 6.9 Hz, 6H). ^{13}C NMR (126 MHz, Chloroform-*d*) δ 171.8, 154.0, 147.5, 141.6, 132.0, 126.2, 123.0, 116.6, 113.4, 79.8, 72.0, 70.6, 70.6, 70.5, 70.5, 70.3, 69.9, 59.0, 38.8, 33.2, 31.9, 29.7, 29.65, 29.59, 29.5, 29.4, 29.3, 25.1, 22.7, 14.1. MS (MALDI-TOF) *m/z*: $[M+Na]^+$ calcd for $C_{92}H_{160}BrN_3NaO_{26}^+$ 1825.037; found 1825.193.

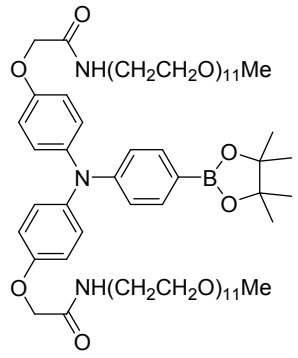

Compound 7a: Under a nitrogen atmosphere, compound **6a** (1.9 g, 1.3 mmol), $Pd(Ph_3P)_2Cl_2$ (90.0 mg, 0.1 mmol), and potassium acetate (0.4 g, 4.0 mmol) were dissolved in dimethylformamide (DMF) (15 mL). Bis(pinacolato)diboron (0.66 g, 2.6 mmol) in 1.0 mL of DMF was added to the reaction and the mixture was stirred at 80 ℃ for 12 h. Upon TLC indicating completion of the reaction, the mixture was washed with saturated $NaHCO_3$ solution and brine. The organic phase was collected, dried, filtered, and purified by flash chromatography on silica gel (DCM:MeOH = 19:1) to obtain **7a** as a light yellow liquid (1.4 g, 73% yield). ^{1}H NMR (500 MHz, Chloroform-*d*) δ 7.60 (d, *J* = 8.5 Hz, 2H), 7.04 (d, *J* = 9.0 Hz, 6H), 6.87 – 6.82 (m, 6H), 4.46 (m, 4H), 3.64 – 3.61 (m, 80H), 3.56 – 3.52 (m, 8H), 3.36 (s, 6H), 1.31 (s, 12H). ^{13}C NMR (126 MHz, Chloroform-*d*) δ 168.2, 153.7, 150.9, 141.6, 135.9, 126.9, 119.6, 115.7, 83.5, 71.9, 70.60, 70.57, 70.52, 70.4, 69.8, 67.8, 59.0, 38.8, 24.8. MS (MALDI-TOF) *m/z*: $[M+Na]^+$ calcd for $C_{74}H_{124}BN_3NaO_{28}^+$ 1536.836; found 1536.174.

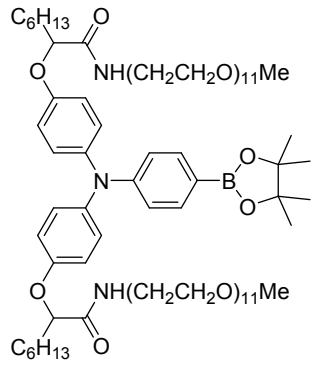

Compound 7b was synthesized using the same method as **7a** and obtained as a light yellow liquid (4.5 g, 72% yield). ^{1}H NMR (500 MHz, Chloroform-*d*) δ 7.54 (d, *J* = 8.3 Hz, 2H), 6.96 (d, *J* = 9.0 Hz, 4H), 6.84 (t, *J* = 5.4 Hz, 2H), 6.81 (d, *J* = 8.3 Hz, 2H), 6.76 (d, *J* = 9.0 Hz, 4H), 4.42 (m, 2H), 3.63 – 3.52 (m, 80H), 3.49 – 3.43 (m, 8H), 3.32 (s, 6H), 1.90 – 1.78 (m, 4H), 1.47 – 1.38 (m, 4H), 1.26 (s, 12H), 1.24 – 1.20 (m, 12H), 0.82 (t, *J* = 6.7 Hz, 6H). ^{13}C NMR (126 MHz, Chloroform-*d*) δ 171.7, 154.0, 150.9, 141.4, 135.8, 126.8, 119.5, 116.5, 83.4, 79.7, 71.9, 70.6, 70.5, 70.5, 70.3, 69.8, 59.0, 38.7, 33.1, 31.6, 29.0, 25.0, 24.8, 22.5, 14.0. MS (MALDI-TOF) *m/z*: $[M+Na]^+$ calcd for $C_{86}H_{148}BN_3NaO_{28}^+$ 1705.024; found 1704.237.

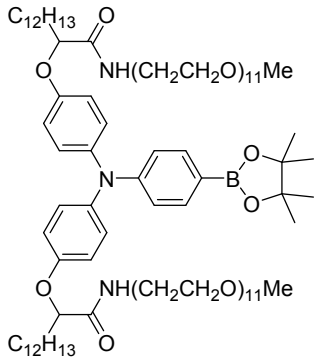

Compound 7c was synthesized using the same method as **7a** and obtained as a light yellow liquid (2.1 g, 70% yield). ^{1}H NMR (500 MHz, Chloroform-*d*) δ 7.58 (d, *J* = 8.4 Hz, 2H), 6.99 (d, *J* = 9.0 Hz, 4H), 6.84 (d, *J* = 8.5 Hz, 4H), 6.79 (d, *J* = 9.0 Hz, 4H), 4.45 (m, 2H), 3.64 – 3.55 (m, 80H), 3.51 – 3.43 (m, 8H), 3.35 (s, 6H), 1.93 – 1.82 (m, 4H), 1.49 – 1.40 (m, 4H), 1.29 (s, 12H), 1.26 – 1.21 (m, 36H), 0.85 (t, *J* = 6.8 Hz, 6H). ^{13}C NMR (126 MHz, Chloroform-*d*) δ 171.8, 154.1, 150.9, 141.4, 135.8, 126.8, 119.6, 116.5, 83.5, 79.8, 71.9, 70.60, 70.56, 70.5, 70.3, 69.9, 59.0, 38.7, 33.2, 31.9, 29.65, 29.63, 29.57, 29.5, 29.4, 29.3, 25.1, 24.8, 22.7, 14.1. MS (MALDI-TOF) *m/z*: $[M+Na]^+$ calcd for $C_{98}H_{172}BN_3NaO_{28}^+$ 1873.212; found 1872.328.

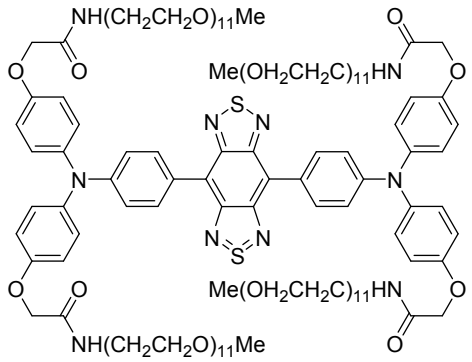

Compound BBT-OEG: Under a nitrogen atmosphere, compound **7a** (1.0 g, 0.7 mmol) and 4,8-Dibromobenzo[1,2-c:4,5-c']bis([1,2,5]thiadiazole) (96.0 mg, 0.3 mmol) were dissolved in 30 mL of 1,4-dioxane and 6 mL of 1 M potassium acetate aqueous solution (1,4-dioxane: H_2O = 5:1). $Pd(dppf)Cl_2$ (48 mg, 65.6 μmol) was then added to the reaction mixture, which was stirred at 80 ℃. After TLC showed the completion of the reaction, the reaction mixture was extracted with DCM, and the organic phase was dried, filtered, and purified by reversed-phase silica gel column chromatography (MeOH:H_2O = 19:1) to obtain **BBT-OEG** as a blue wax (245.0 mg, 30% yield). ^{1}H NMR (500 MHz, Chloroform-*d*) δ 8.14 (d, *J* = 8.7 Hz, 4H), 7.19 (d, *J* = 8.9 Hz, 8H), 7.12 (d, *J* = 8.5 Hz, 8H), 6.90 (d, *J* = 8.9 Hz, 8H), 4.49 (s, 8H), 3.66 – 3.60 (m, 160H), 3.57 – 3.52 (m, 16H), 3.36 (s, 12H). ^{13}C NMR (126 MHz, Chloroform-*d*) δ 168.2, 154.0, 152.7, 148.7, 141.4, 132.7, 127.5, 127.3, 120.0, 119.6, 115.9, 71.9, 70.6, 70.6, 70.5, 70.3, 69.8, 67.8, 59.0, 38.8. MS (MALDI-TOF) *m/z*: $[M+Na]^+$ calcd for $C_{142}H_{224}N_{10}NaO_{52}S_2^+$ 2988.453; found 2987.118.

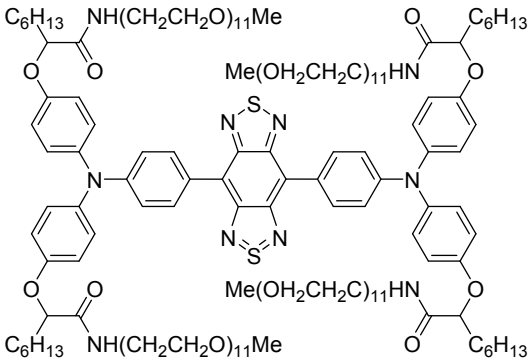

Compound BBT-C6 was synthesized using the same method as **BBT-OEG** and obtained as a green wax (71.0 mg, 43% yield). ^{1}H NMR (500 MHz, Chloroform-*d*) δ 8.12 (d, *J* = 8.4 Hz, 4H), 7.14 (d, *J* = 8.5 Hz, 8H), 7.09 (d, *J* = 8.5 Hz, 4H), 6.89 – 6.84 (m, 12H), 4.48 (m, 4H), 3.62 – 3.59 (m, 160H), 3.53 – 3.50 (m, 16H), 3.34 (s, 12H), 1.93 – 1.83 (m, 8H), 1.49 – 1.41 (m, 8H), 1.32 – 1.22 (m, 24H), 0.85 (t, *J* = 6.6 Hz, 12H). ^{13}C NMR (126 MHz, Chloroform-*d*) δ 171.8, 154.4, 152.7, 148.7, 141.2, 132.7, 127.4, 127.3, 120.0, 119.5, 116.6, 79.8, 71.9, 70.6, 70.54, 70.49, 70.3, 69.9, 59.0, 38.8, 33.1, 31.6, 29.0, 25.0, 22.6, 14.1. MS (MALDI-TOF) *m/z*: $[M+Na]^+$ calcd for $C_{166}H_{272}N_{10}NaO_{52}S_2^+$ 3324.829; found 3323.334.

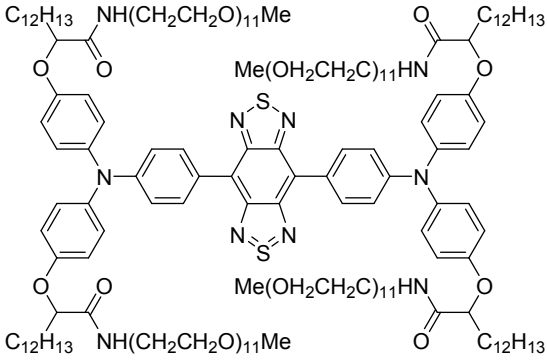

Compound BBT-C12 was synthesized using the same method as **BBT-OEG** and obtained as a green wax (144.0 mg, 25% yield). ^{1}H NMR (500 MHz, Chloroform-*d*) δ 8.14 (d, *J* = 8.5 Hz, 4H), 7.15 (d, *J* = 8.6 Hz, 8H), 7.11 (d, *J* = 8.7 Hz, 4H), 6.91 (t, *J* = 5.5 Hz, 4H), 6.87 (d, *J* = 8.7 Hz, 8H), 4.49 (m, 4H), 3.66 – 3.58 (m, 160H), 3.55 – 3.51 (m, 18H), 3.36 (s, 12H), 1.94 – 1.84 (m, 8H), 1.51 – 1.43 (m, 8H), 1.29 – 1.22 (m, 72H), 0.86 (t, *J* = 6.8 Hz, 12H). ^{13}C NMR (126 MHz, Chloroform-*d*) δ 171.8, 154.4, 152.7, 148.8, 141.2, 132.7, 127.4, 127.3, 120.0, 119.5, 116.6, 79.8, 71.9, 70.59, 70.55, 70.5, 70.3, 69.9, 59.0, 38.8, 33.2, 31.9, 29.7, 29.65, 29.60, 29.5, 29.4, 29.4, 25.2, 22.7, 14.1. MS (MALDI-TOF) *m/z*: $[M+Na]^+$ calcd for $C_{190}H_{320}N_{10}NaO_{52}S_2^+$ 3661.204; found 3659.280.

4. Experimental Section

4.1 Absorbance and fluorescence measurements

BBT-OEG and **BBT-C6** were dissolved in H_2O, and **BBT-C12** was dissolved in methanol to prepare solutions at concentrations: 100, 50, 25, 12.5, 6.3, and 3.1 μM, respectively. UV absorption spectra of these three compounds at various concentrations were measured with water or methanol serving as controls (Figure S1). The absorbance at the maximum excitation wavelength was plotted against concentration (Figure S10d). Linear fitting was performed using Origin 2024.

Fluorescence emission spectra of **BBT-OEG**, **BBT-C6**, and **BBT-C12** at concentrations of 100, 50, 25, 12.5, 6.3, and 3.1 μM, were recorded using a NIR-II fluorescence spectrometer, with excitation at 808 nm and a slit width of 5 nm.

Fluorescence intensities of **BBT-OEG** and **BBT-C6** solutions with different water (poor solvent)/methanol (good solvent) ratios were utilized to investigate the aggregation-induced emission (AIE) characteristics. **BBT-OEG** and **BBT-C6** were initially prepared in a stock solution at a concentration of 300 μM using methanol as the solvent. Solutions with varying water content (0%, 10%, 20%, 30%, 40%, 50%, 60%, 70%, 80% and 90%) were then prepared by diluting the stock solution accordingly. These solutions were placed into fluorescence cuvettes, and their fluorescence spectra were measured using a NIR-II fluorescence spectrometer with an excitation wavelength of 808 nm and a slit width of 5 nm.

4.2 Critical micelle concentration (CMC) determination

The CMC of **BBT-OEG** and **BBT-C6** was determined using pyrene as a probe. Briefly, 3.0 mg of pyrene was dissolved in 5 mL of acetone, and then 0.1 mL of the pyrene stock solution was diluted with acetone to a total volume of 5 mL. The resulting solution was aliquoted into Eppendorf tubes and left overnight for acetone to evaporate.

BBT-OEG and **BBT-C6** were prepared in a stock solution at a concentration of 200 μM using H_2O as the solvent. These stock solutions were further diluted to prepare solutions at concentrations of 200 μM, 100 μM, 80 μM, 60 μM, 40 μM, 30 μM, 20 μM, 10 μM, 5 μM, 4 μM, 3 μM, 2 μM, and 1 μM. Each diluted solution (1 mL each) was added to the corresponding pyrene-containing Eppendorf tubes. The mixtures were sonicated for 30 minutes, followed by incubation in a 60°C water bath for 40 minutes, and then left at room temperature for 12 hours. The fluorescence intensity of each solution was measured with an excitation wavelength of 334 nm and a slit width of 5 nm. The fluorescence intensities, I_{373} and I_{384}, of the pyrene emission spectrum in each solution were measured at wavelengths 373 nm and 384 nm, respectively. The ratio I_{373}/I_{384} was calculated for each concentration. A

concentration ratio curve was plotted to determine the CMC of the compounds, identified as the turning point in the curve.

4.3 *n*-Octanol/water partition coefficients (Log P) determination

The *n*-octanol/water partition coefficients (LogP) values of **BBT-OEG**, **BBT-C6**, and **BBT-C12** were determined using the shake-flask method[17]. The calibration curve for each compound in water-saturated *n*-octanol was plotted using UV–Vis spectrophotometry (Shimadzu UV-2600) (Figure S2). Each compound was weighed and dissolved in 2 mL of water-saturated *n*-octanol to prepare solutions at concentrations of 50 μM, 25 μM, and 12.5 μM, and 2 mL of water saturated with *n*-octanol was added, respectively. The mixture was shaken at 37 ^{o}C and 120 rpm for 24 h. Subsequently, 0.6 mL of the *n*-octanol phase was transferred and analyzed using the calibration curve method. The log P values were calculated using the following equation: LogP = Lg[(Co)/(Cs-Co)], where Co is the concentration of the compound in the *n*-octanol phase, and Cs is the starting concentration of the compound in the *n*-octanol solution.

4.4 Evaluation of photothermal properties

Photothermal properties: **BBT-OEG** or **BBT-C6** was dissolved in water to prepare solutions at concentrations of 100 μM, 80 μM, 60 μM, 40 μM, 20 μM, 10 μM, and 5 μM. Each solution (1 mL) was transferred into an Eppendorf tube and irradiated under an 808 nm laser (1.0 W/cm^2) for 10 minutes. The laser spot diameter on the sample was 1.0 cm. The real-time temperature of the samples was recorded using a near-infrared thermal imager every 30 seconds, with water used as a control.

Photothermal stability: A sample with a concentration of 40 μM was irradiated under an 808 nm laser (1.0 W/cm^2), after which the laser was turned off. The temperatures of the sample solutions were recorded every 30 seconds using a near-infrared thermal imager during five cycles of heating and cooling progress. In one heating-cooling circle, the 808 nm laser was first used to irradiate the samples for 10 min, then the laser was removed, and the samples were naturally cooled down to ambient temperature in 16 min.

Determination of photothermal conversion efficiency[18]: A sample with a concentration of 30 μM was irradiated under an 808 nm laser for 10 minutes, then recording the sample temperature every 30 seconds until it naturally cooled down to ambient temperature. The photothermal conversion efficiency (η) of the sample can be calculated according to the following equation.

$$\eta = \frac{hS(T_{Max} - T_{Surr}) - Q_{dis}}{I(1 - 10^{-A_\lambda})} \qquad (1)$$

Where *h* is the heat transfer coefficient, S is the surface area of the container, T_{max} is the equilibrium temperature, T_{surr} is the ambient temperature (23.9 ℃), I is the laser power used for the photothermal experiment (1.0 W/cm^2) A_λ is the absorbance at the used laser wavelength (808 nm), and η is the photothermal transduction efficiency.

The value of hS can be obtained using the following equation.

$$hS = \frac{m_W C_W}{\tau_s} \qquad (2)$$

where m_w is the mass of water (0.5 g), C_w is the heat capacity of water (4.2 J/g), τ_s is the sample system time constant. To determine τ_s, a dimensionless driving force temperature θ is introduced, which is defined by the following equation.

$$t = \tau_s(-ln\theta) \qquad (3)$$

$$\theta = \frac{T_{surr} - T}{T_{surr} - T_{Max}} \qquad (4)$$

Where T is the real-time temperature of the sample when the laser was turned off, t represents the time.

4.5 Light stability experiment

Aqueous solution samples containing **BBT-C6** at a concentration of 20 μM were prepared. 1 mL of each sample was loaded into the Eppendorf tube. The samples were irradiated under an 808 nm laser (1 W/cm²) for durations of 0 min, 10 min, 20 min, 30 min, 40 min, 50 min, and 60 min, respectively. Subsequently, the samples irradiated with the laser were subjected to UV–Vis spectrophotometry analysis. The absorbance at the maximum absorption wavelength was recorded, with the absorbance of the sample before laser irradiation set as 1 for reference. The ratio of the absorbance after laser irradiation to the absorbance before laser irradiation was observed to assess the light stability of the samples. The experimental data were plotted using Origin 2024 software, with ICG serving as the control group.

4.6 Characterization of BBT@DOX

Dynamic light scattering (DLS) measurement was performed to determine the average hydrodynamic size and the zeta potential of **BBT@DOX** using Malvern Zetasizer (Malvern, Nano ZS 90, UK). Data were given as mean ± standard deviation (SD) based on three independent measurements.

Transmission electron microscopy (TEM, JEM-2100, JEOL) was used to observe the morphology of **BBT@DOX**. Samples were prepared by dropping 5 μL of the solution on 230 mesh carbon support films (copper mesh) and kept at room temperature for 2 h without disturbing. The excess liquid was then absorbed employing a

filter paper, and stained with 1% phosphotungstic acid solution for 30 seconds before taking images.

4.7 Encapsulation efficiency and drug loading content

Encapsulation efficiency (EE%) and drug loading content (DLC%) of nanoemulsions **BBT@DOX** were determined using high-performance liquid chromatography (HPLC, Shimadzu LC-20A, an Amethyst C18-H reversed-phase column was used, particle size 5.0 μm, column dimension 4.6 × 250 mm). A calibration curve for doxorubicin (DOX) in methanol was first plotted using HPLC.

4.8 *In vitro* drug release

The drug release profile of **BBT@DOX** was studied using the dialysis method and assessed by UV–Vis absorbance. Initially, a calibration curve for doxorubicin hydrochloride (DOX·HCl) in water was plotted using UV–Vis spectrophotometry (Evolution 200, Thermo).

2 mL of nanoemulsions **BBT@DOX** was placed in a dialysis bag (membrane cut off: 1 kDa). The dialysis bags were sealed and immersed in PBS buffer at pH 5.5 and 7.4, respectively. The solutions were then placed in an incubator at 37.0 ± 0.5 °C and shaking at 120 rpm. At specified intervals (0.5 h, 1 h, 2 h, 3 h, 4 h, 6 h, and 8 h), 1 mL of dialysate was withdrawn. A fresh buffer solution of the same volume and temperature was immediately added, and the absorbance of the withdrawn dialysate was measured at 480 nm using UV-Vis spectrophotometry. The cumulative percentage of drug release was calculated accordingly.

4.9 Cell culture

The human lung adenocarcinoma cell line (A549) was purchased from Beyotime (Shanghai, China), Human normal lung epithelial cell line (BEAS-2B) was purchased from Wuhan Xavier Biotechnology Co., LTD. Human lung adenocarcinoma cell/DOX-resistant strain A549/DOX was purchased from Shanghai Fuyu Biotechnology Co., LTD. The cells were cultured in a cell incubator at 37 °C and 5% CO_2 using DMEM (high glucose) medium supplemented with 10% (v/v) fetal bovine serum and 1% (v/v) penicillin-streptomycin.

4.10 Cytotoxicity assays

The cytotoxicity of **BBT-C6** and **BBT@DOX** against A549 and A549/DOX cells was evaluated using a cell counting kit assay (CCK-8, Beyotime, China). The cell viabilities were all calculated using the following equation:

$$\text{Cell viability} = \frac{OD_{sample} - OD_{blank}}{OD_{control} - OD_{blank}} \times 100\%$$

To determine the synergistic effect between photothermal therapy and chemotherapy, the combination index

(CI) was calculated[19] using the following equation:

$$CI = \frac{C_A}{IC_{50A}} + \frac{C_B}{IC_{50B}}$$

where C_A and C_B denote the doses of agents **DOX** and **BBT-C6** in **BBT@DOX** respectively, as the combination reached a 50% proliferation inhibitory rate; IC_{50A} and IC_{50B} denote the doses of single agents **DOX** and **BBT-C6** under a 50% proliferation inhibitory rate. CI < 1 is considered to indicate synergistic effects of the two combined agents.

4.11 Cell death staining

A549 cells were seeded into 20 mm confocal dishes at a density of 1 × 10^5 cells per dish. After 24 hours of adherent culture, the old medium was removed. DMEM containing DOX, **BBT-C6**, and **BBT@DOX** (with DOX concentration of 8 μg/mL and **BBT-C6** concentration of 30 μM) was added, respectively. After incubating for 12 h, cells were irradiated with an 808 nm laser (1.0 W/cm²) for 10 minutes and incubated for another 12 h. Cells were washed with cold PBS three times, and then stained using the Calcein-AM/PI double staining kit, followed by imaging with a laser confocal microscope (A1R/A1, Nikon).

4.12 Hemolytic test

First, red blood cells (RBC) were separated by centrifugation (1400 rpm, 5 min) and washed with PBS (pH 7.4) 4 times until the supernatant became clear. RBC suspension in 0.3 mL PBS was then mixed with 0.3 mL **BBT@DOX** (**BBT-C6** concentrations: 0.5, 1.0, 5.0, 10.0, 20.0, 40.0, 60.0, 80.0, and 100.0 μM). PBS and water were used as negative and positive controls, respectively. Then, the obtained suspension was cultured at 37 °C for 3 h and centrifuged to observe the color of the supernatant. Finally, the absorption of the supernatant was measured at 541 nm using an ultraviolet spectrophotometer.

4.13 Western blotting

A549 or A549/DOX cells were seeded in 6-well plates at the density of 5 × 10^5 cells per well and incubated overnight. The suspension in the wells was replaced by fresh medium containing DOX (18 μM), BBT-2 (18 μM), or **BBT@DOX** (DOX concentraion: 18 μM), and cells were cultured for another 12 h. Then, the total protein of cells was extracted by RIPA lysis buffer. About 30 mg of cell lysate mixed with 5 x SDS-PAGE loading buffer was heated for 10 min at 95 °C. The samples were subjected to SDS-PAGE gel for electrophoresis and then the gels were transferred to poly(vinylidenedifluoride) membranes. 5% skim milk dissolved in Tris-Buffered Saline-Tween-20 (TBST) was used to block the PVDF membranes for 0.5 h. Subsequently incubation overnigh tat 4 °C with primary

antibodies, then washing for another 3 times with TBST before the HRP-conjugated secondary antibodies were added. β-Actin was used to confirm equal loading in each lane in the samples prepared from cell lysates.

4.14 Tumor model

Briefly, a xenograft tumor model was established in nude mice (female, 20 ± 2 g, 5-6 weeks old) by injecting either A549 or A549/DOX cells (5×10^6 cells in 100 μL PBS) into the right hind flank. The length (L) and width (W) of each tumor were measured, and the tumor volume (V) was calculated using the following formula: $V=L\times W^2\times0.5$.

5. $^{1}H/^{13}C$ NMR and MALDI-TOF MS Spectra of Compounds.

^{1}H NMR spectra of compound **2**

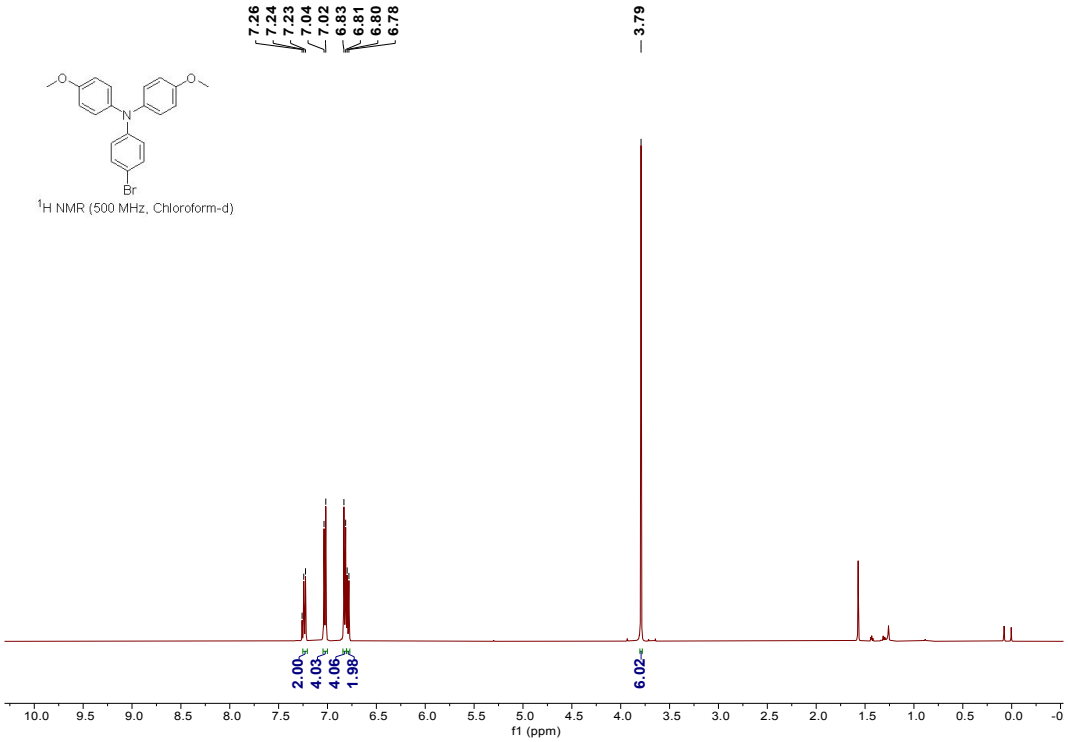

^{1}H NMR spectra of compound **3**

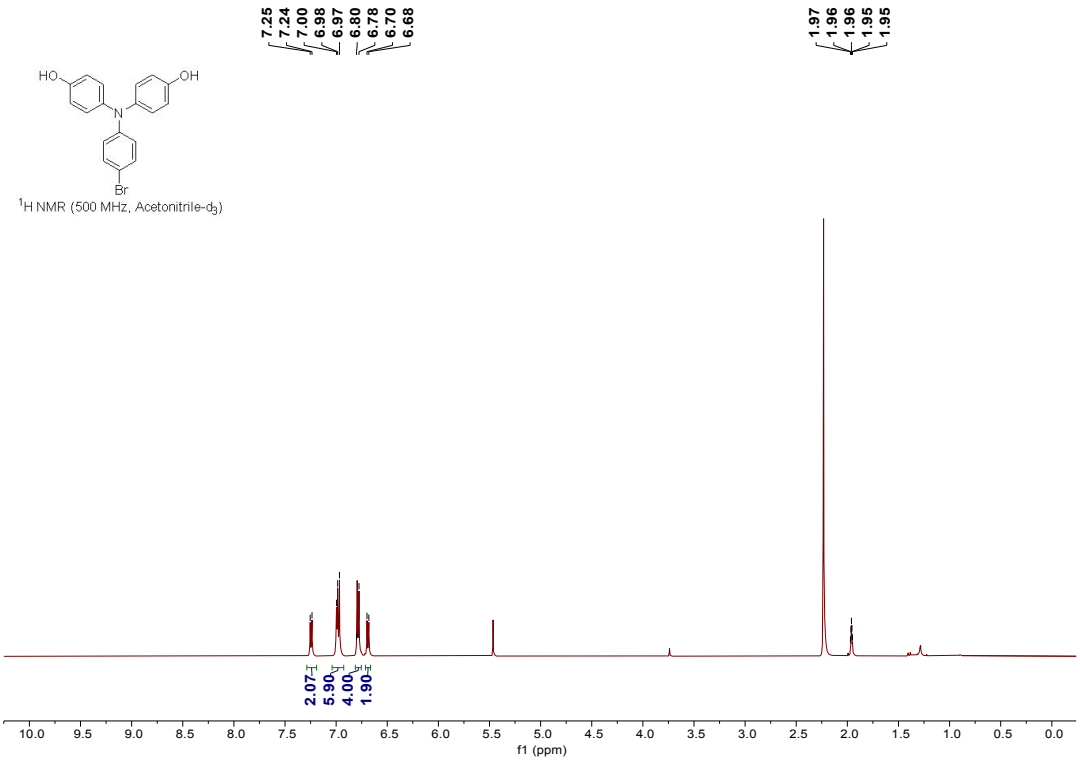

^{1}H NMR spectra of compound **4a**

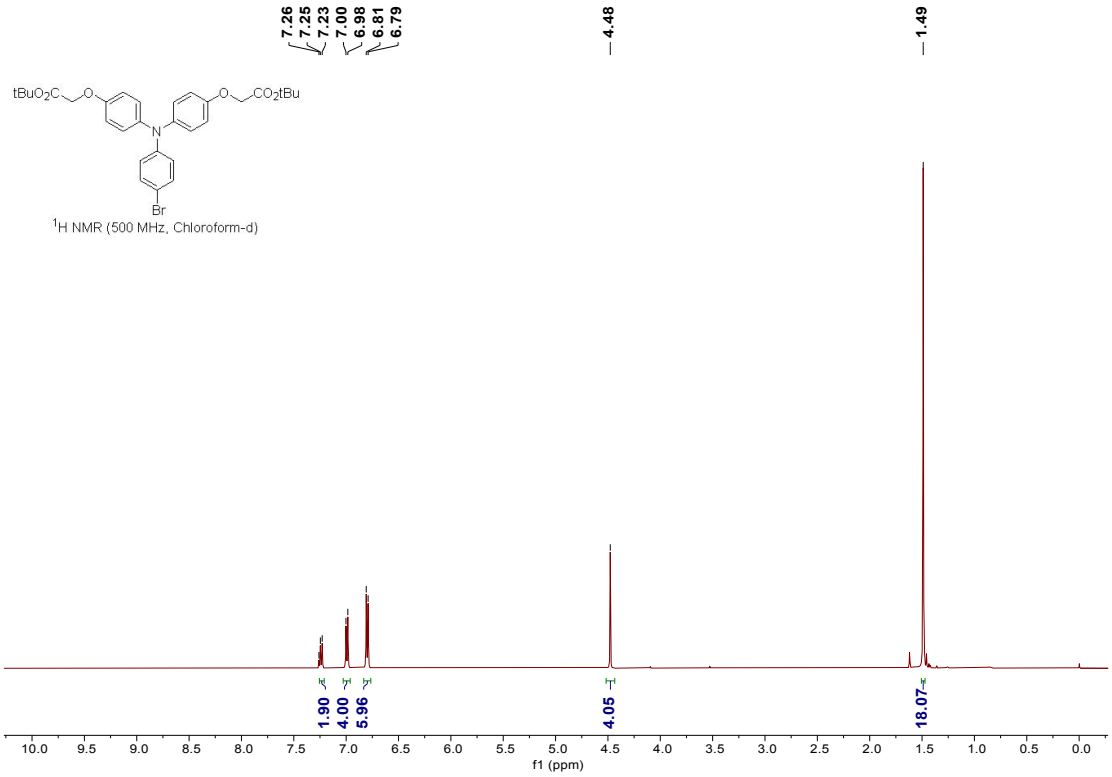

^{13}C NMR spectra of compound **4a**

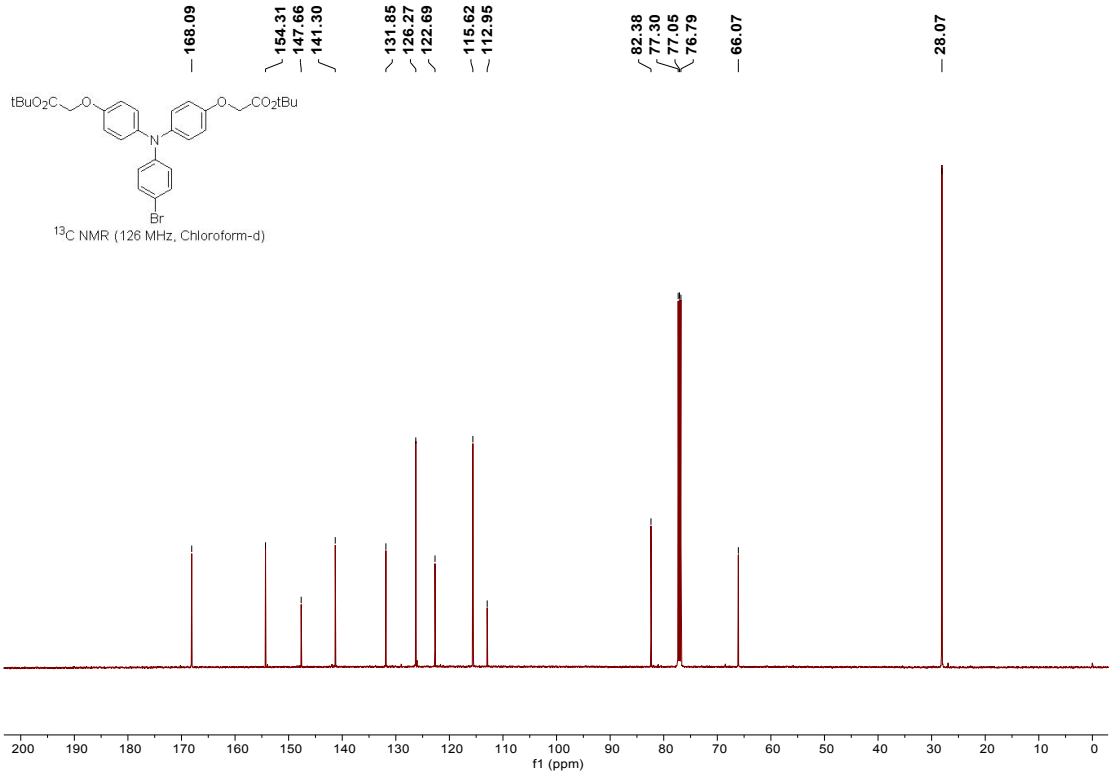

MALDI-TOF MS of compound **4a**

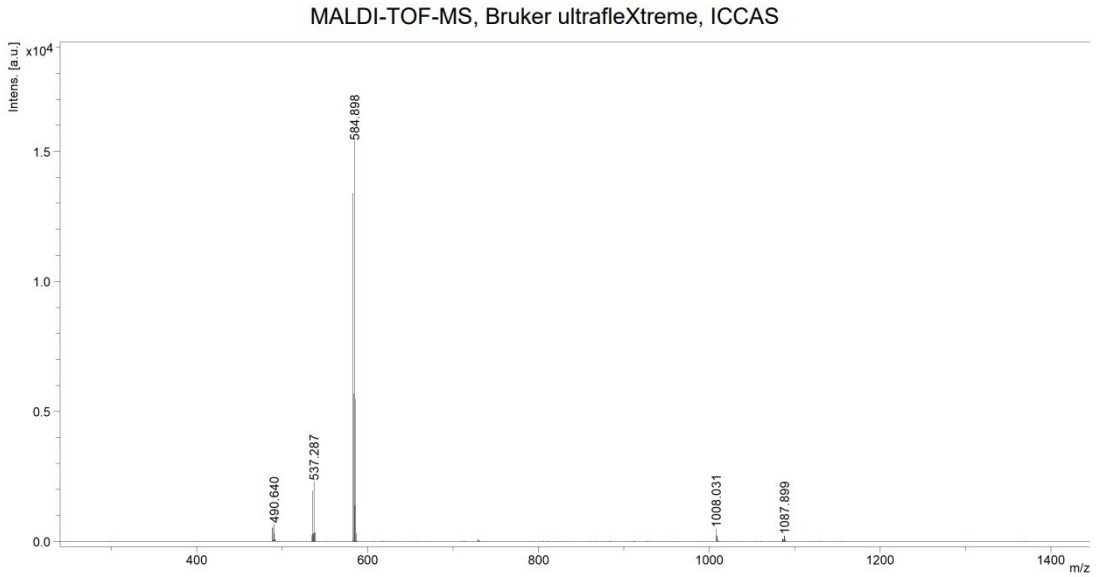

^{1}H NMR spectra of compound **4b**

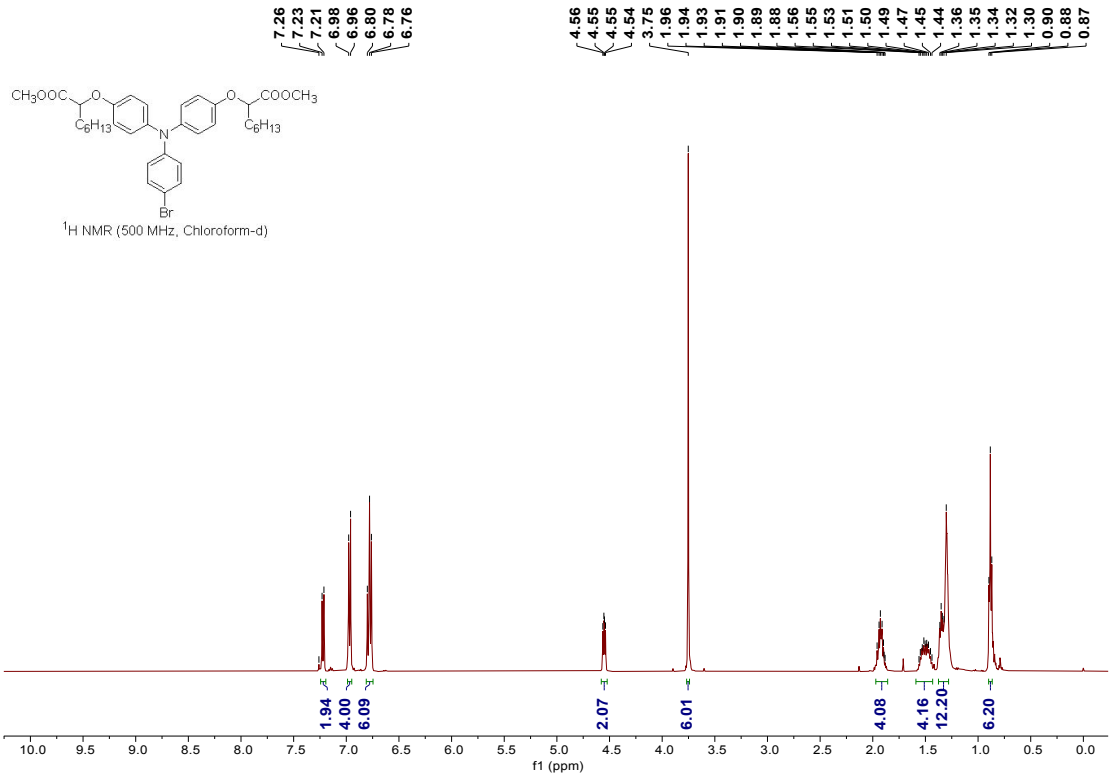

^{13}C NMR spectra of compound **4b**

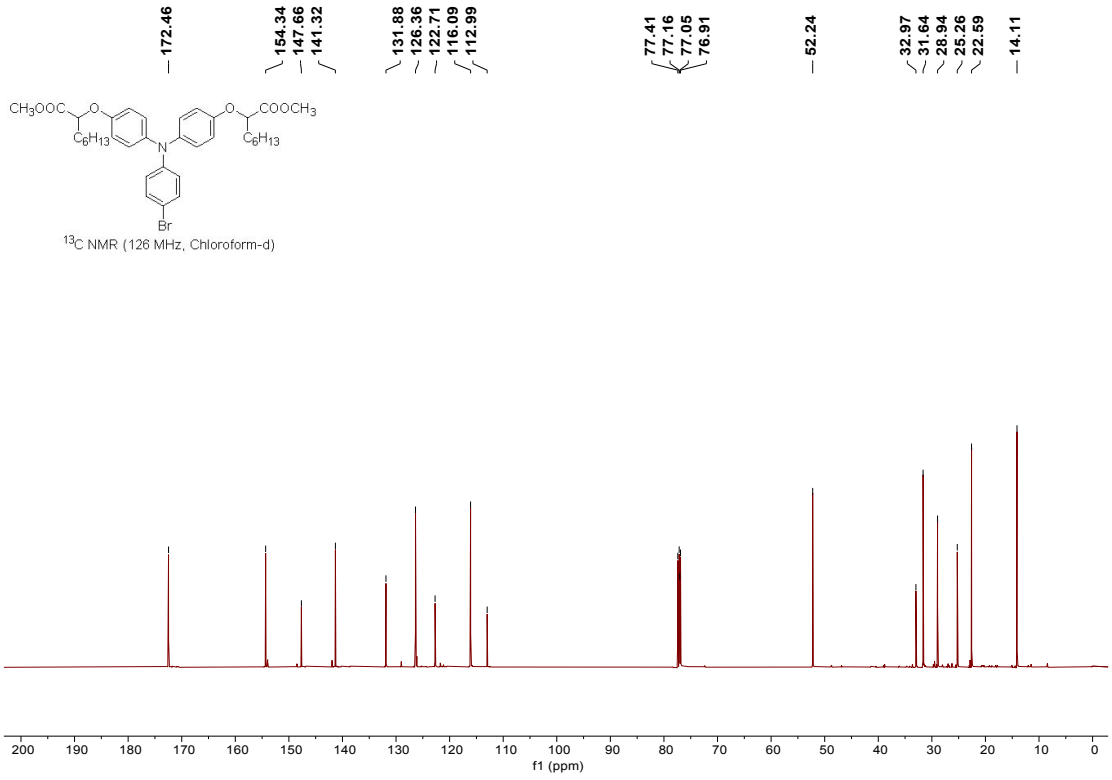

MALDI-TOF MS of compound **4b**

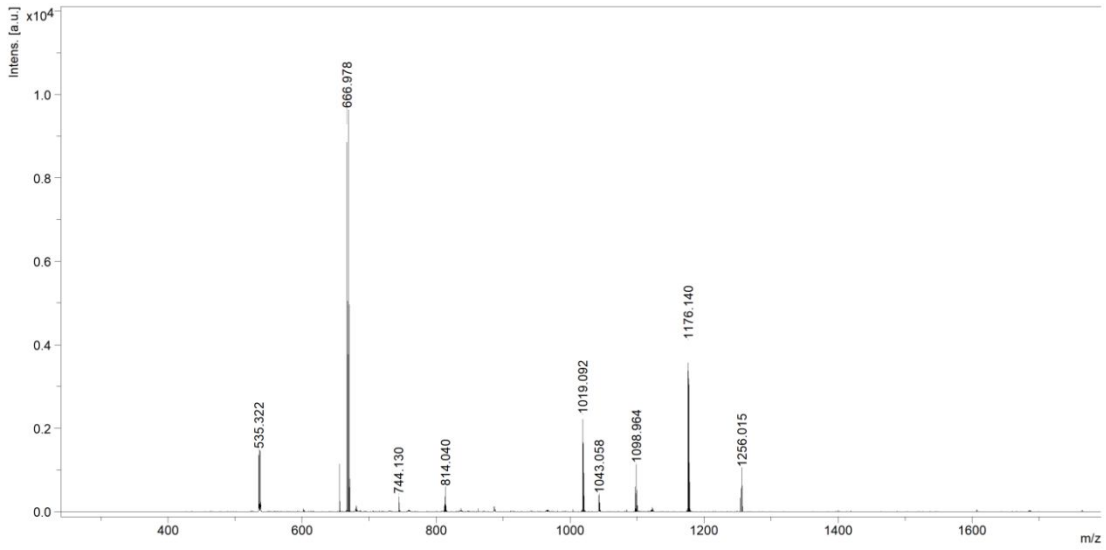

^{1}H NMR spectra of compound **4c**

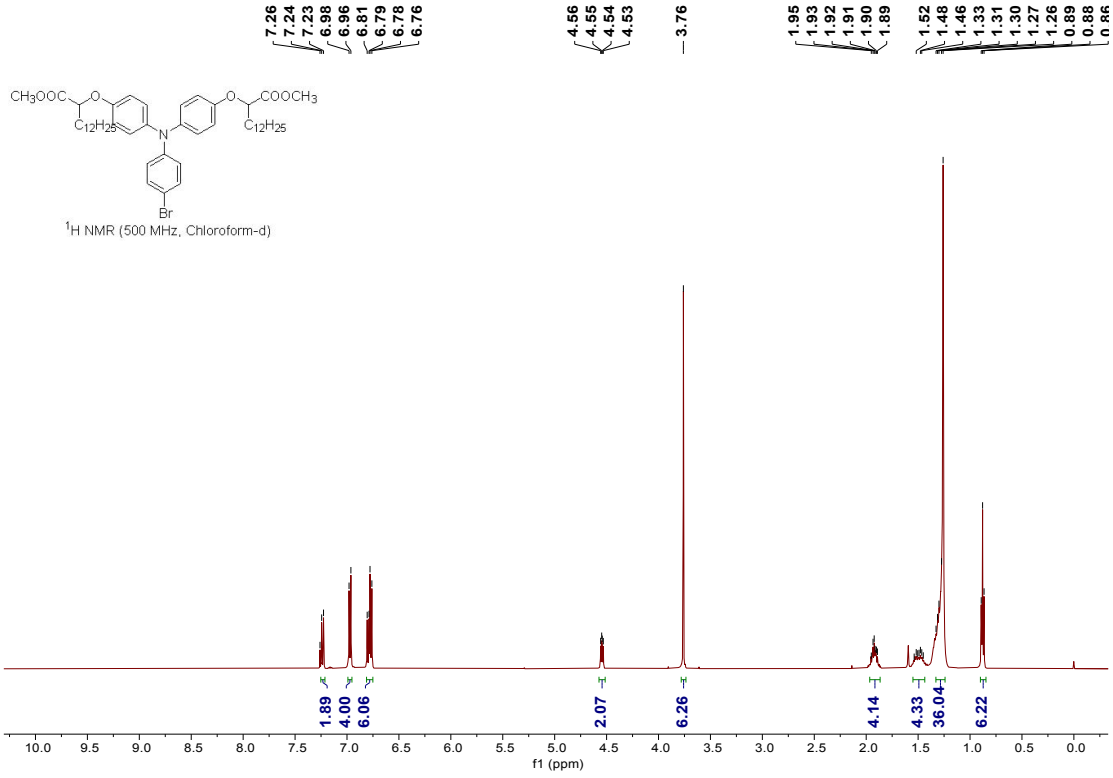

^{13}C NMR spectra of compound **4c**

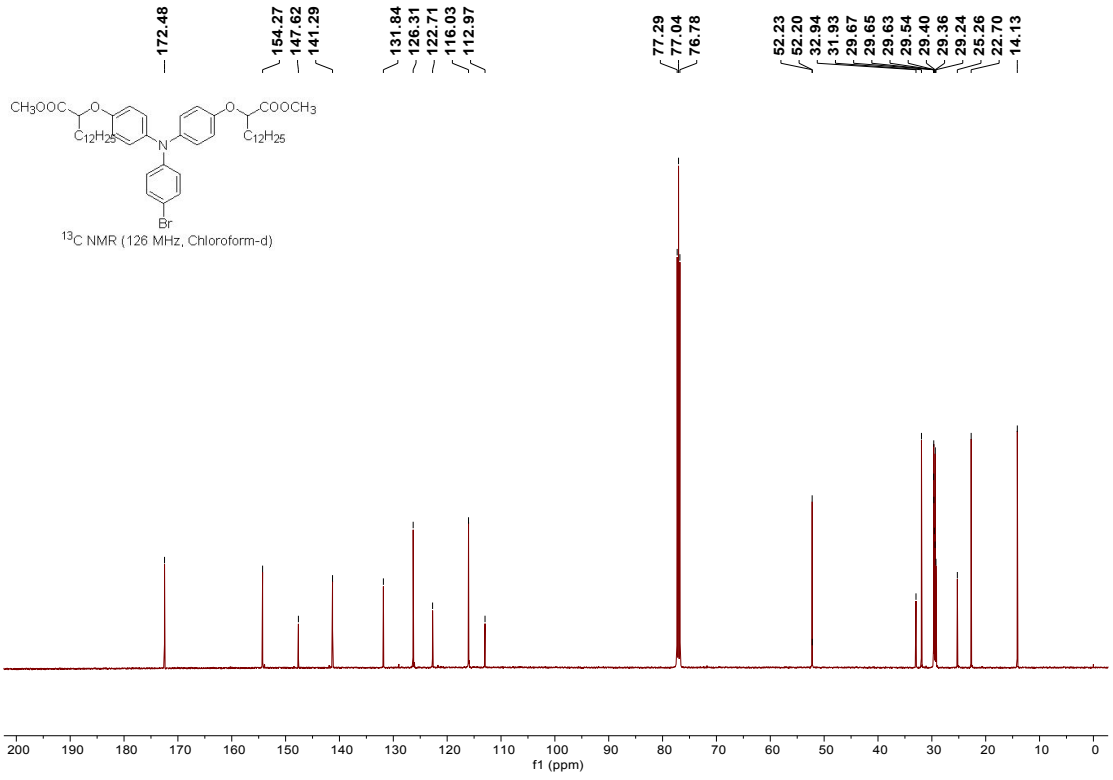

MALDI-TOF MS of compound **4c**

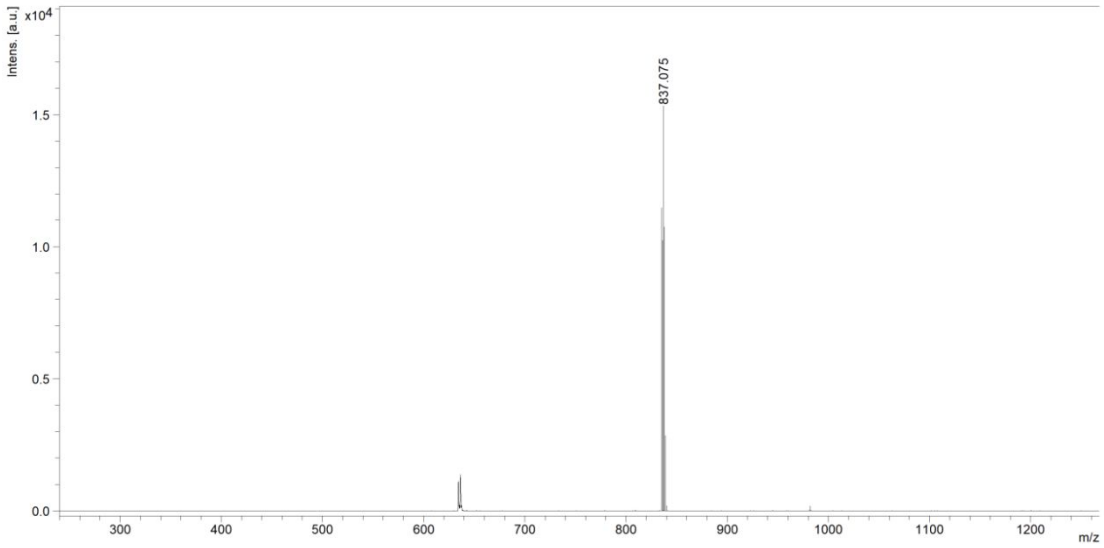

^{1}H NMR spectra of compound **6a**

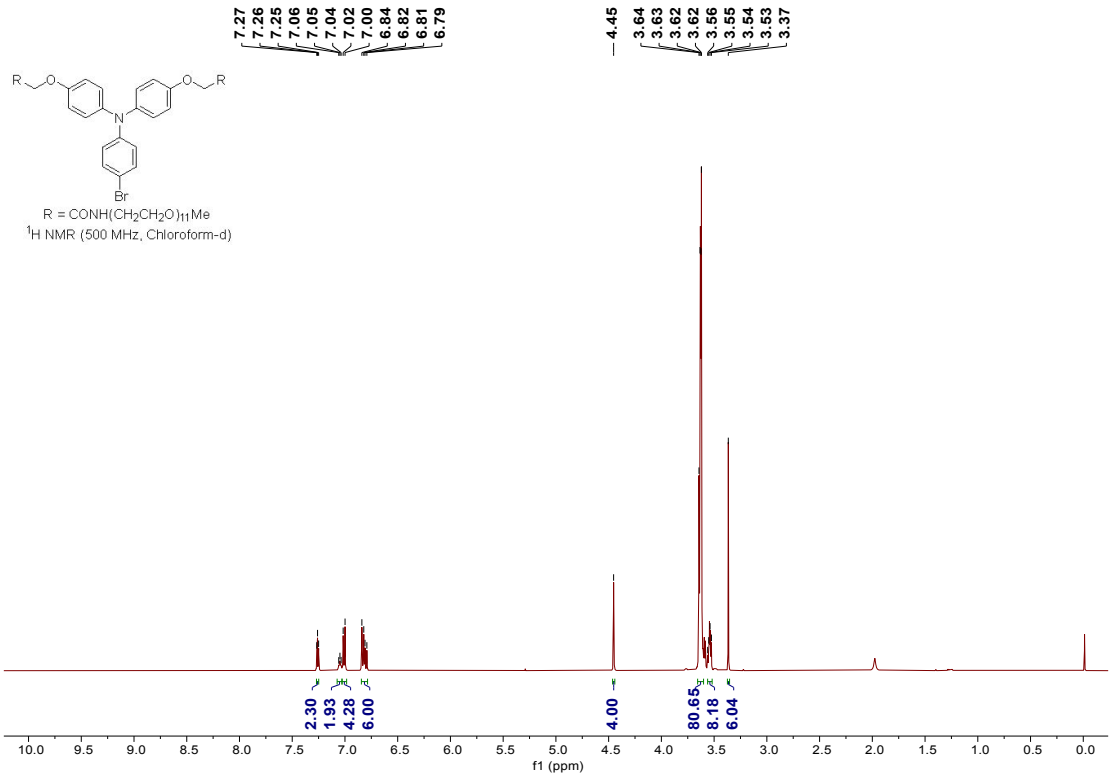

^{13}C NMR spectra of compound **6a**

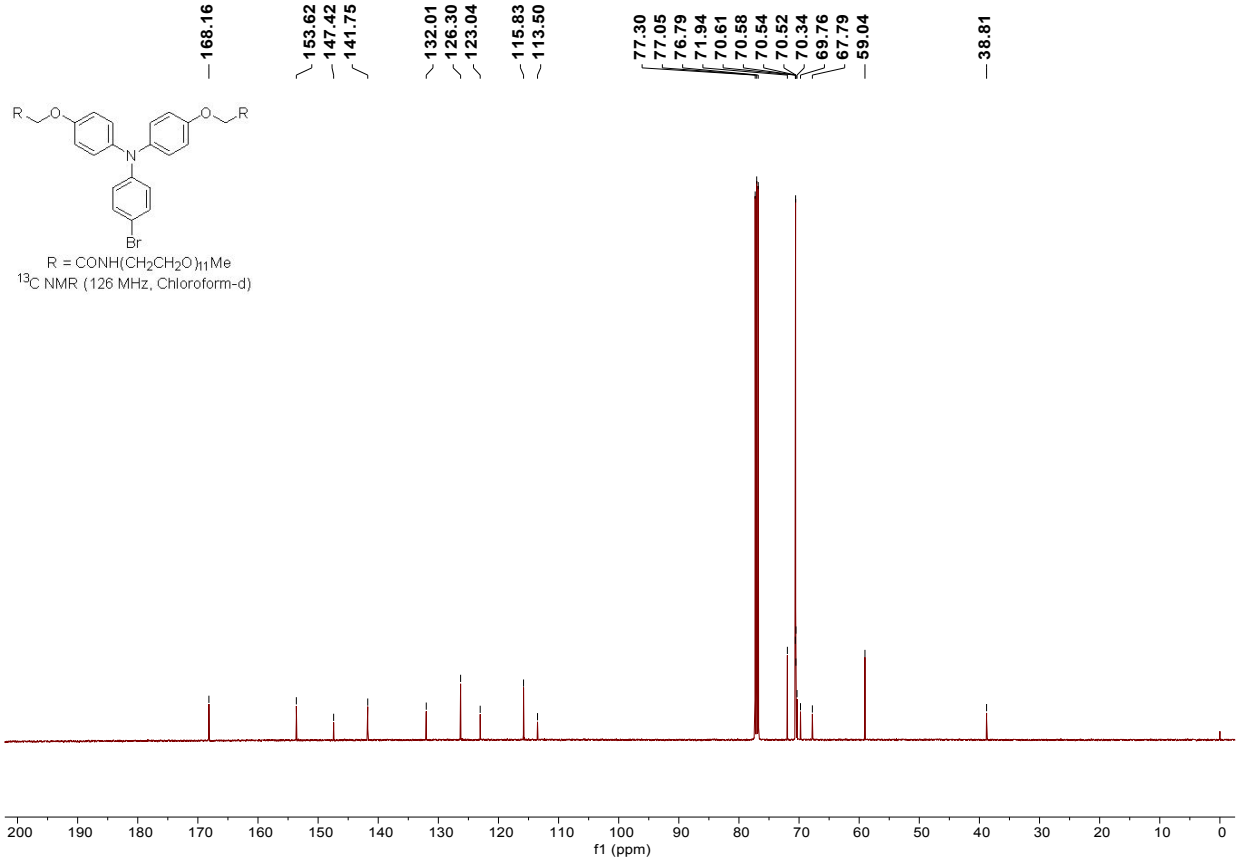

MALDI-TOF MS of compound **6a**

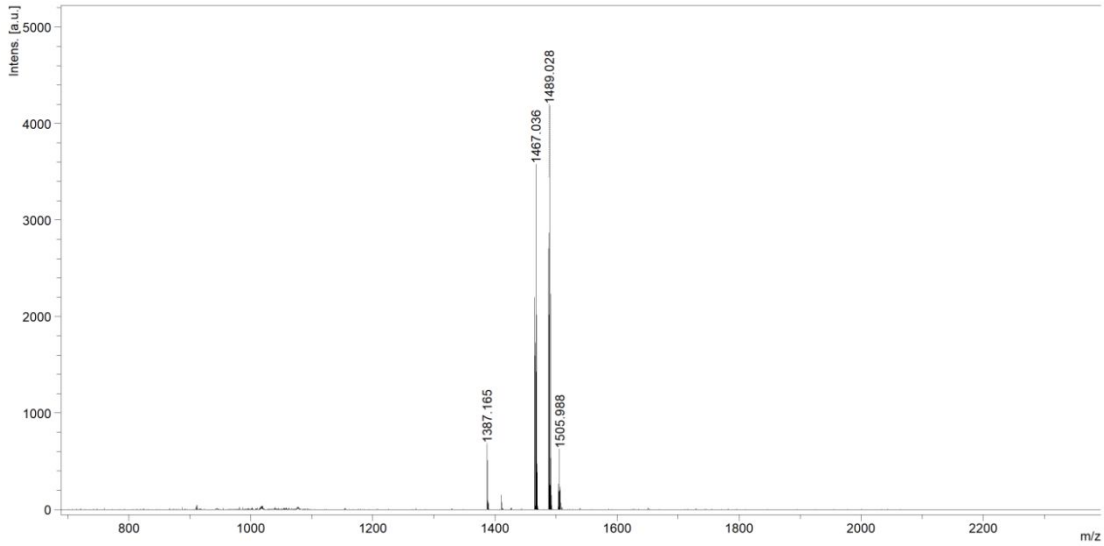

^{1}H NMR spectra of compound **6b**

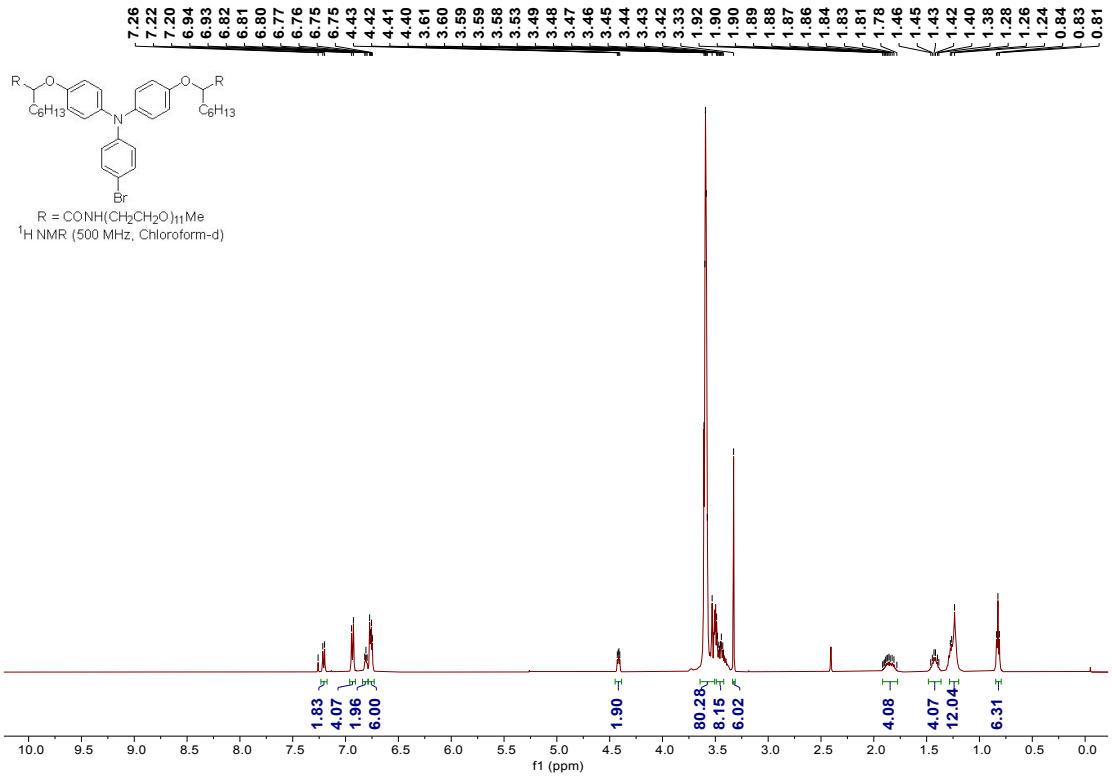

^{13}C NMR spectra of compound **6b**

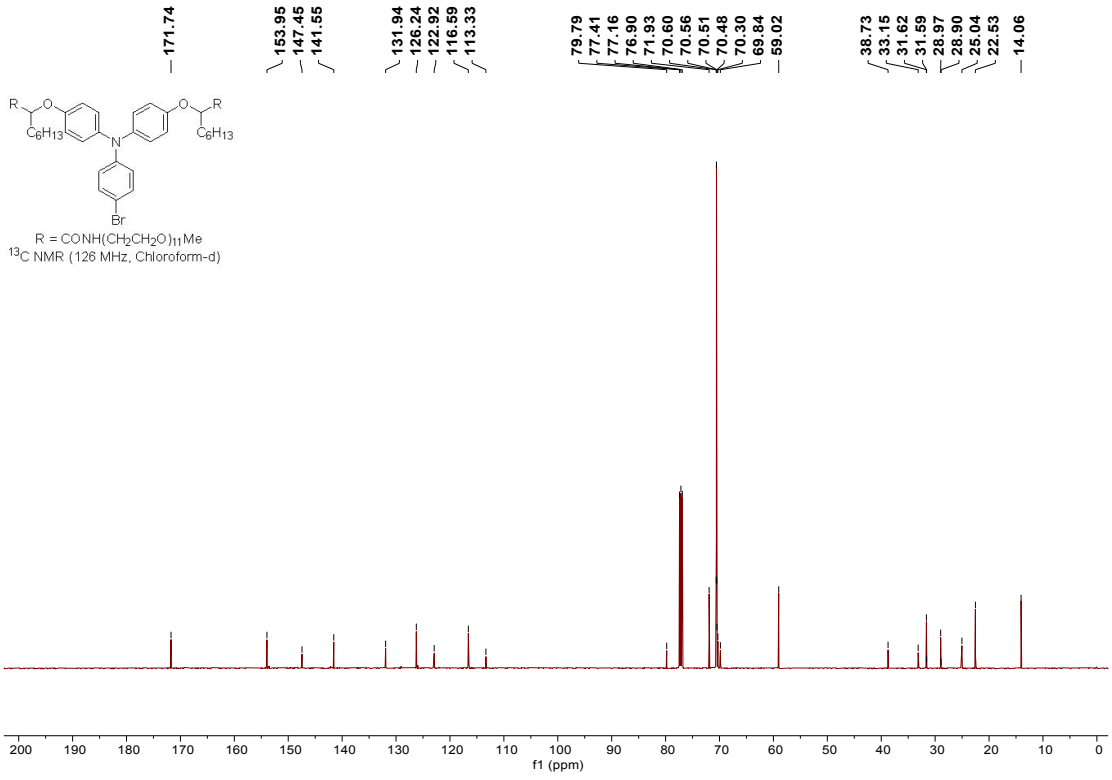

MALDI-TOF MS of compound **6b**

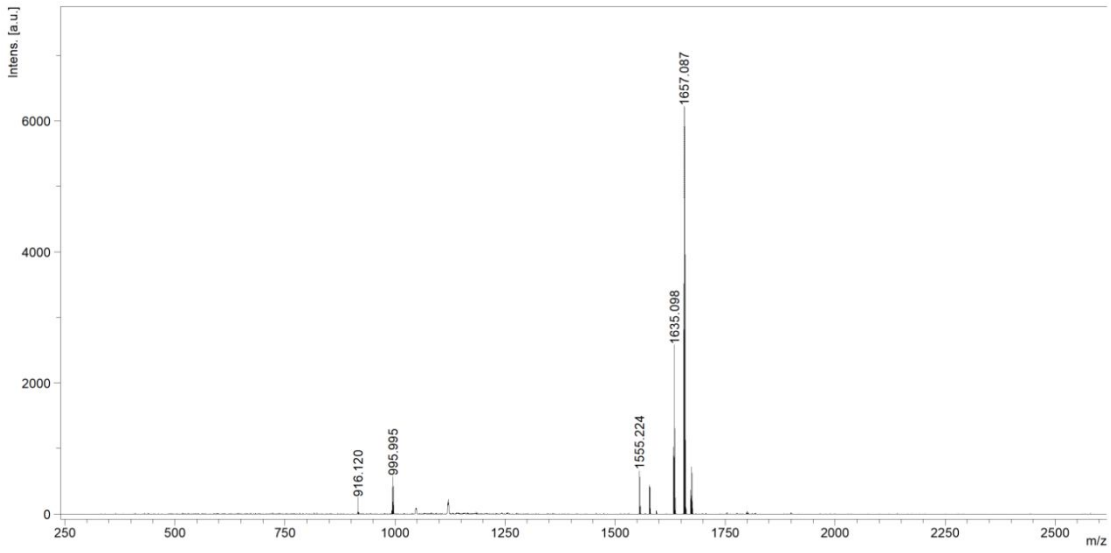

^{1}H NMR spectra of compound **6c**

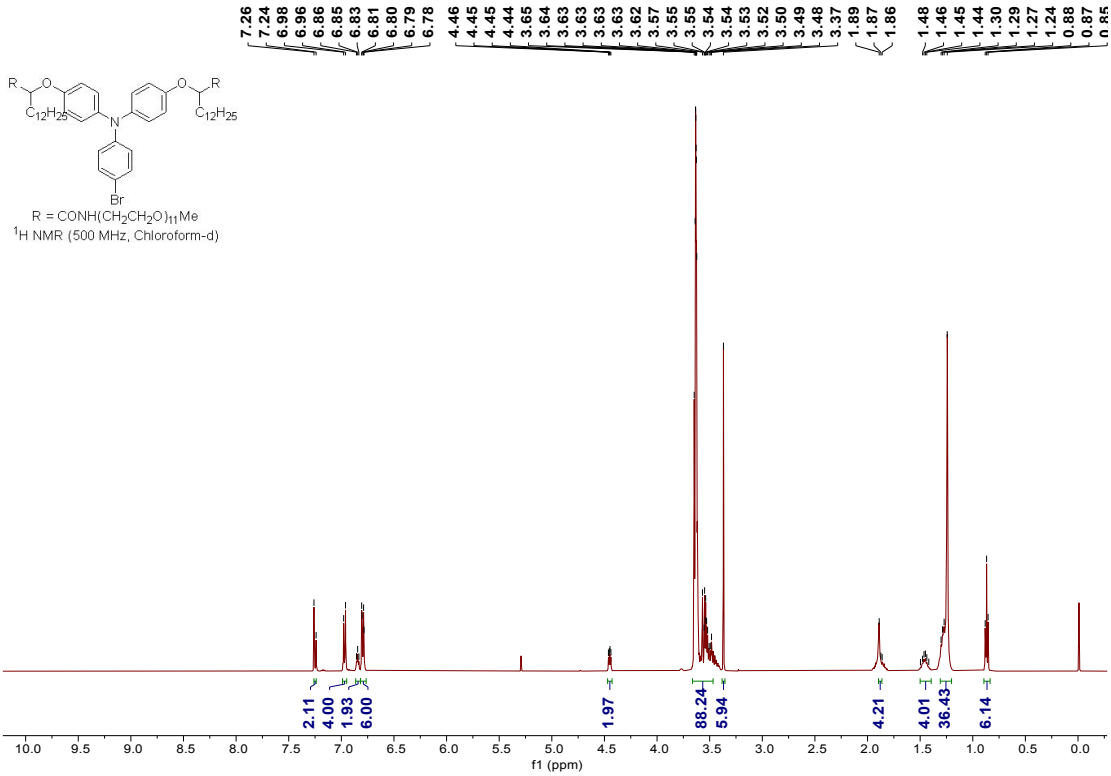

^{13}C NMR spectra of compound **6c**

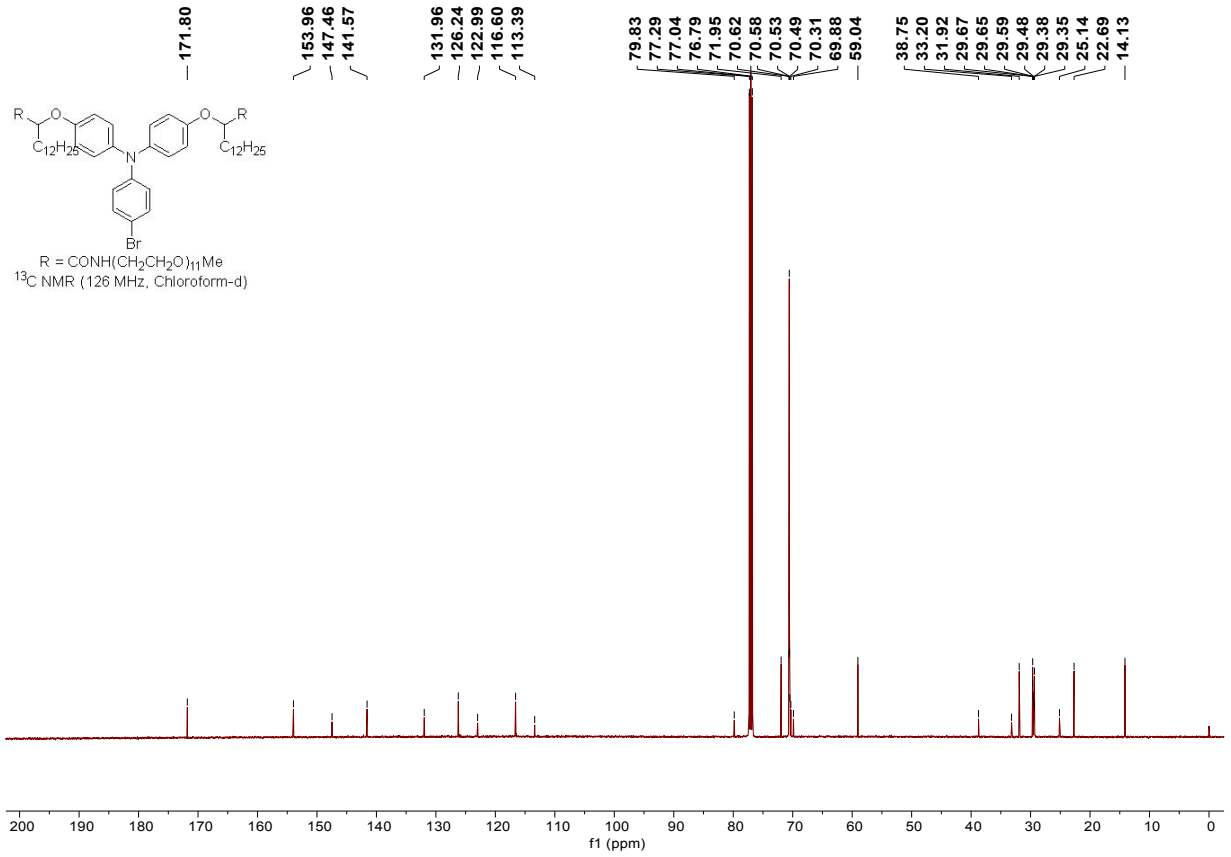

MALDI-TOF MS of compound **6c**

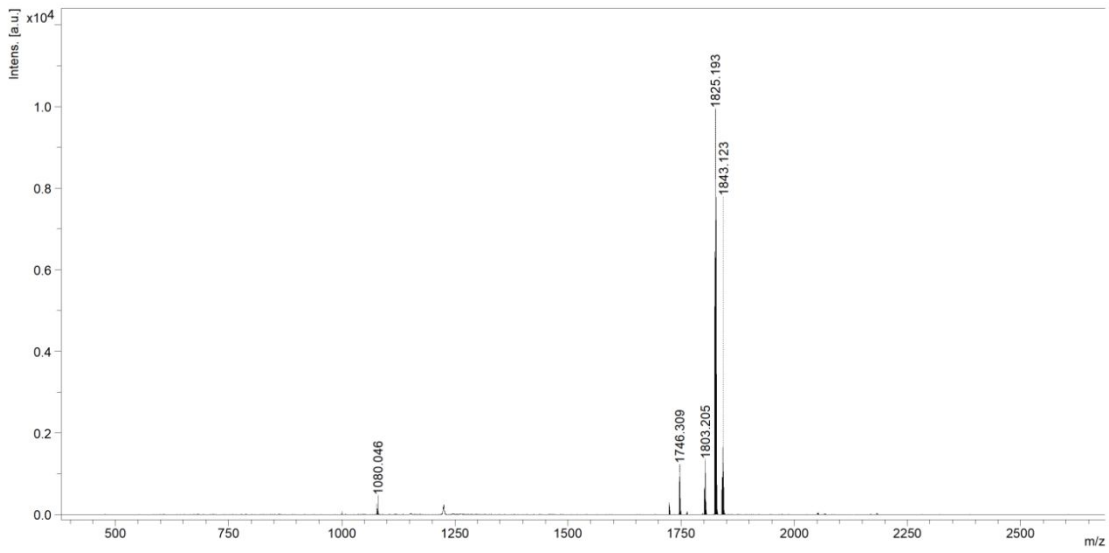

^{1}H NMR spectra of compound **7a**

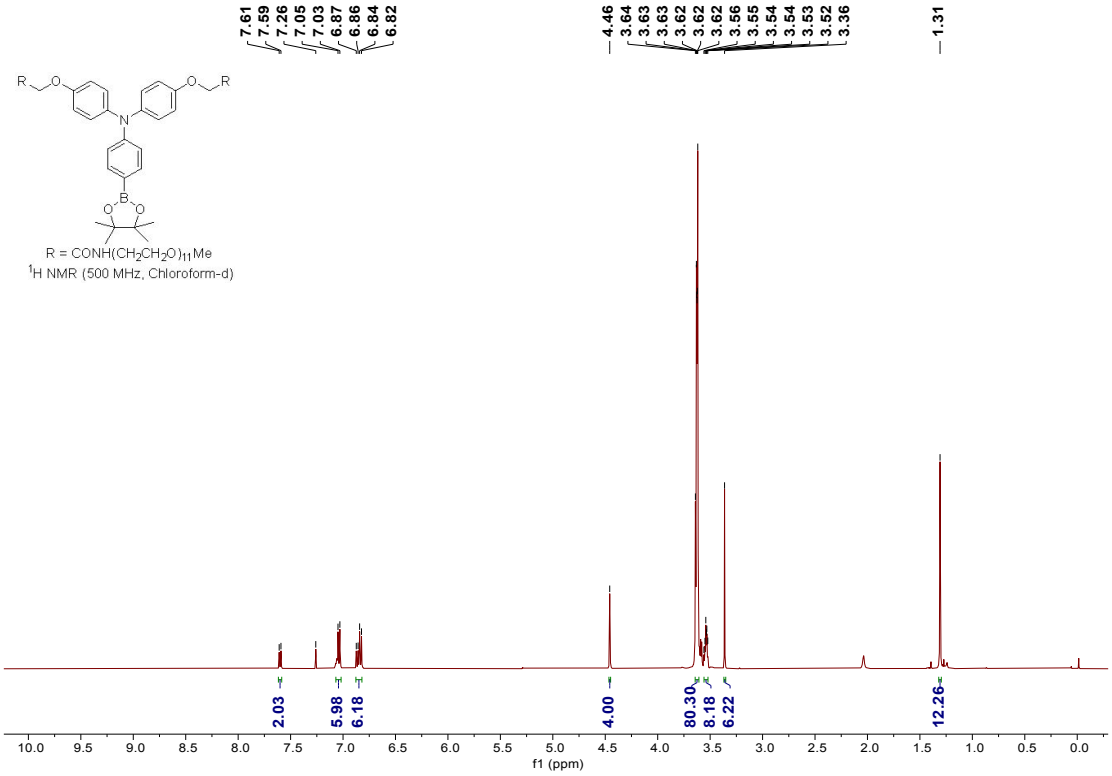

^{13}C NMR spectra of compound **7a**

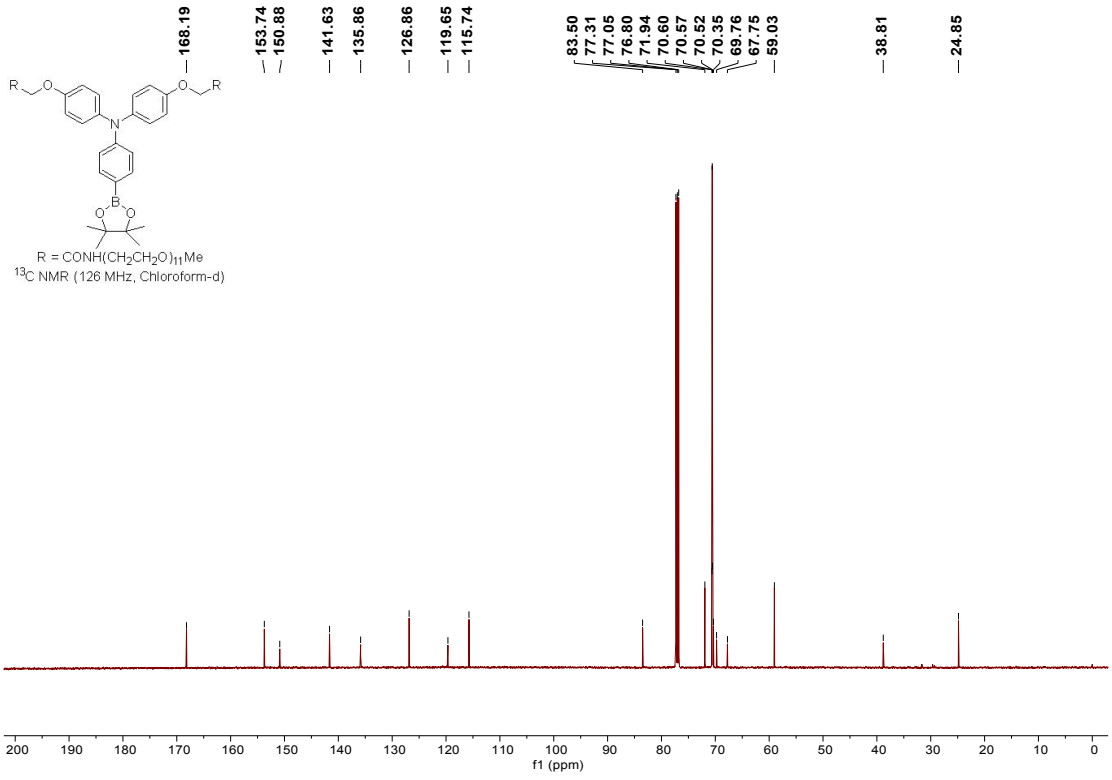

MALDI-TOF MS of compound **7a**

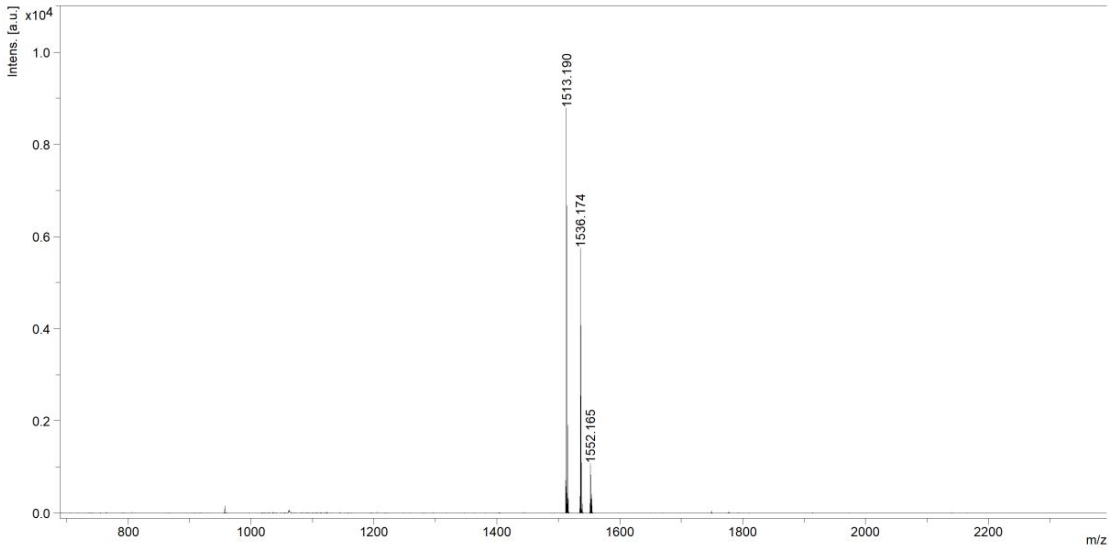

^{1}H NMR spectra of compound **7b**

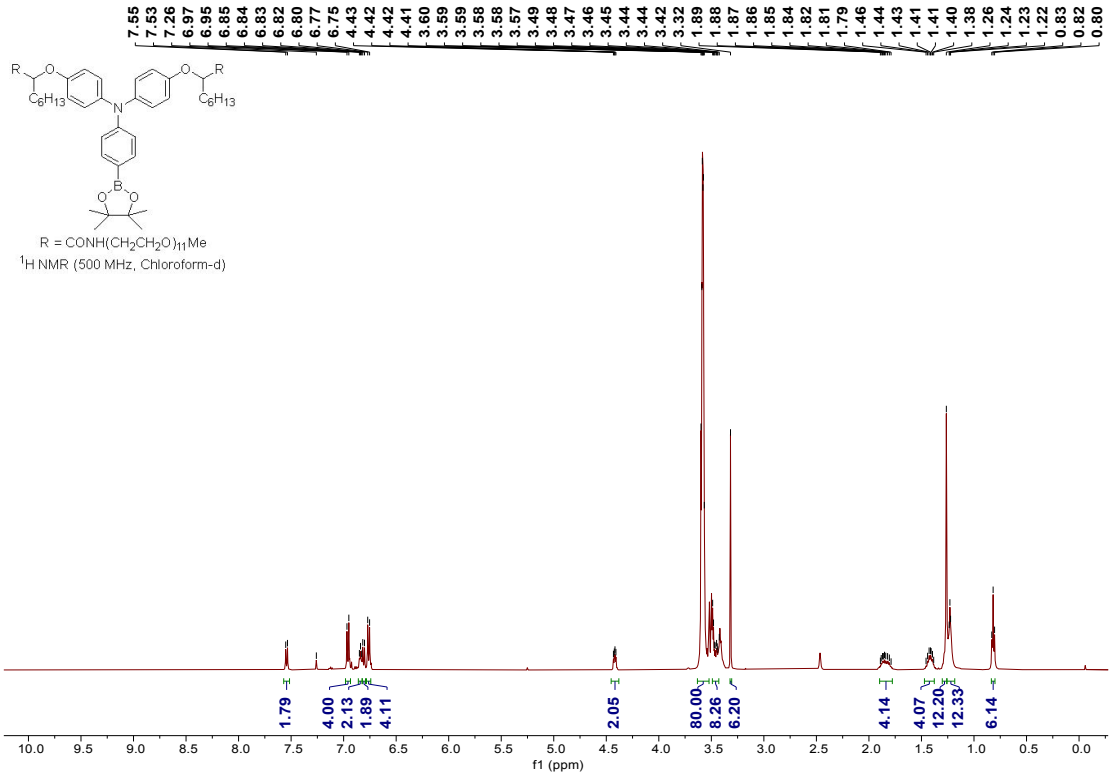

^{13}C NMR spectra of compound **7b**

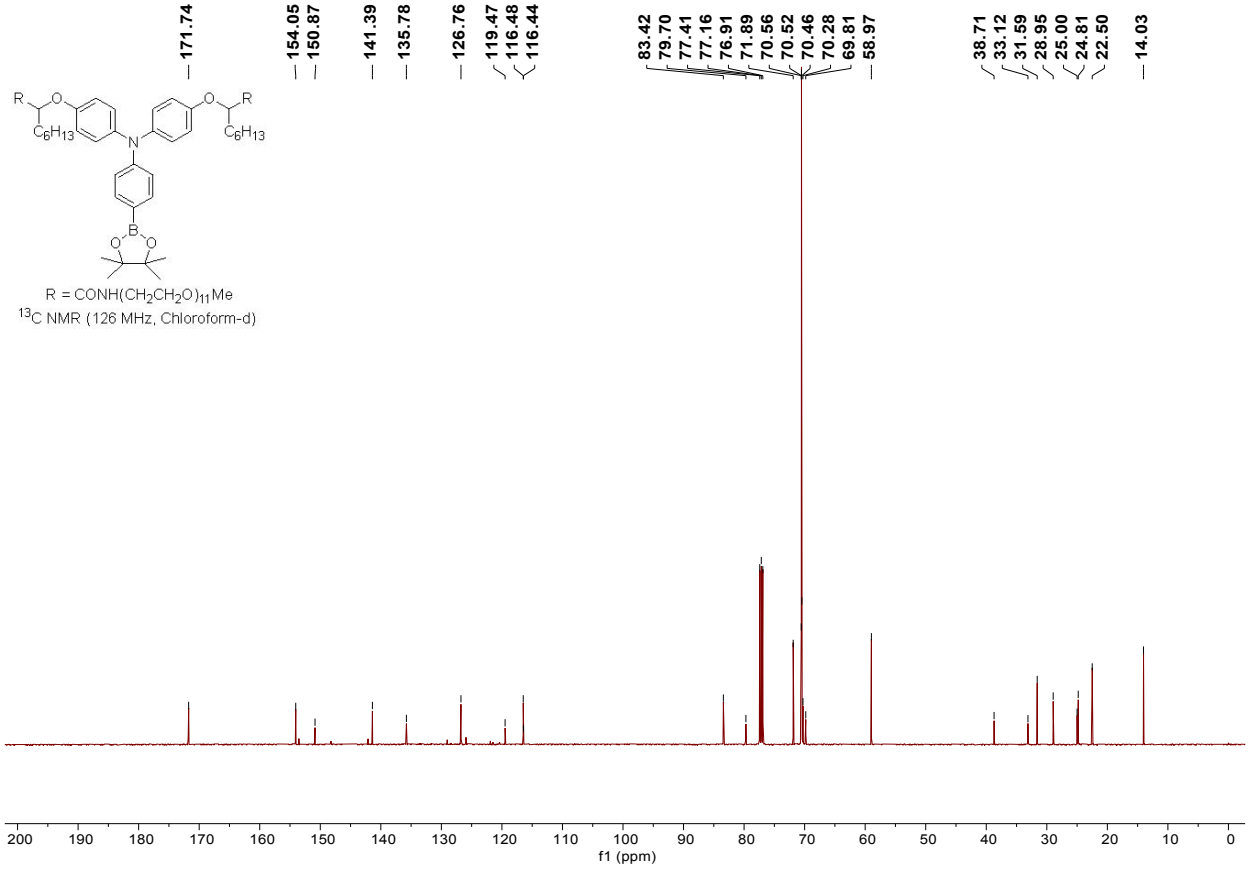

MALDI-TOF MS of compound **7b**

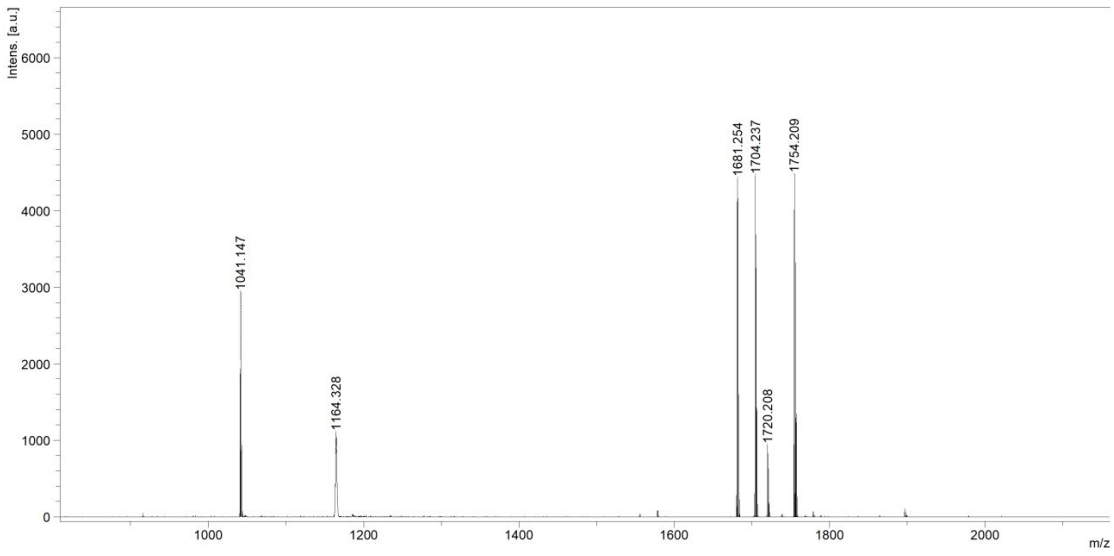

^{1}H NMR spectra of compound **7c**

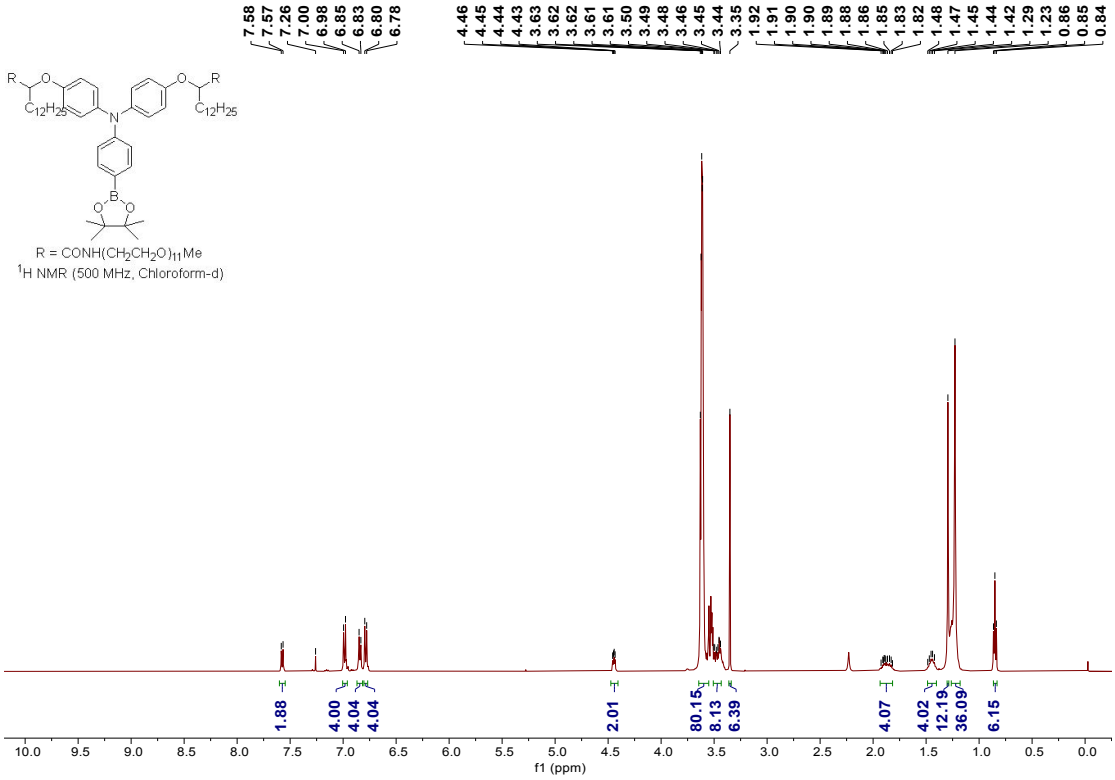

^{13}C NMR spectra of compound **7c**

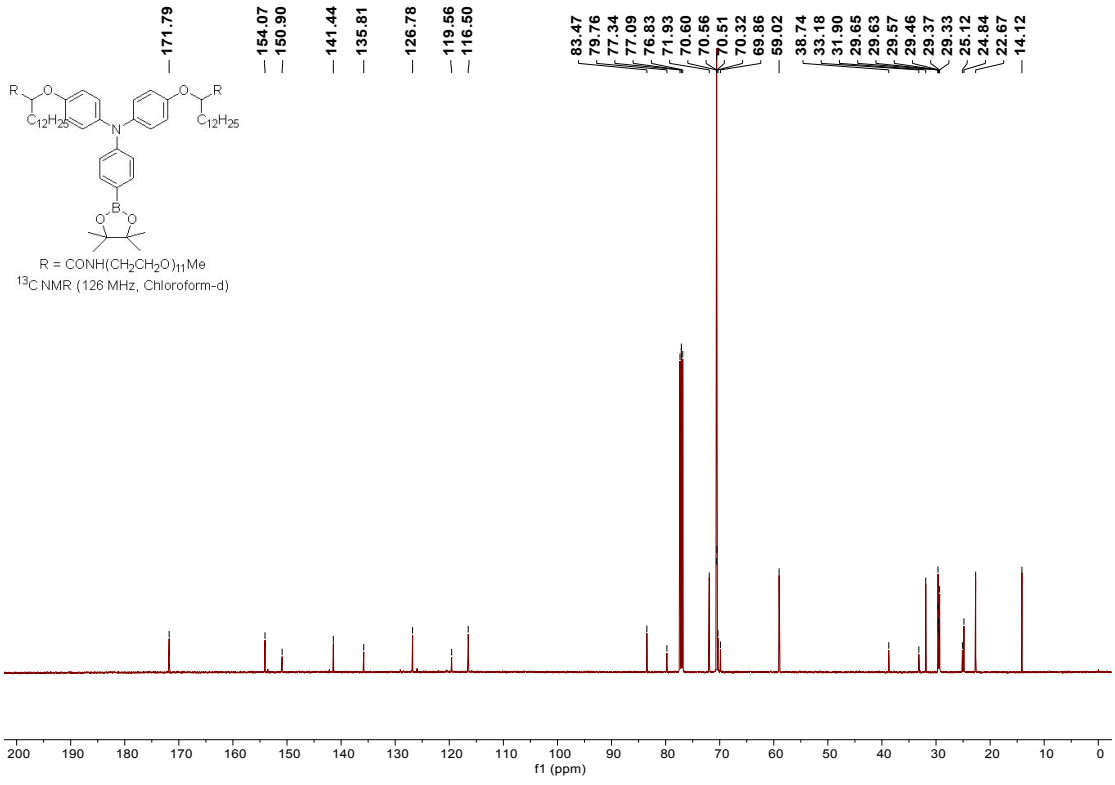

MALDI-TOF MS of compound **7c**

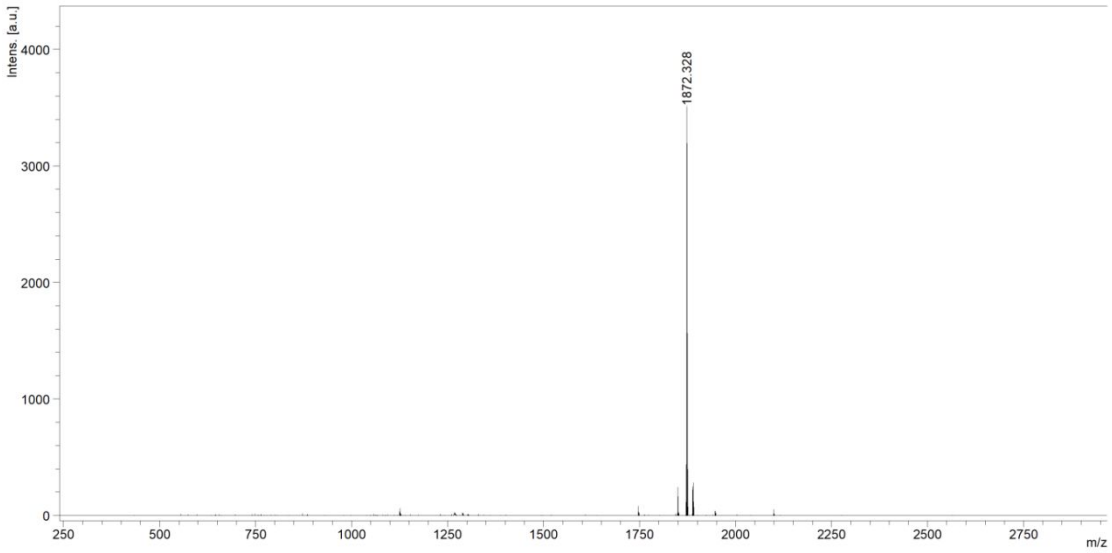

^{1}H NMR spectra of compound **BBT-OEG**

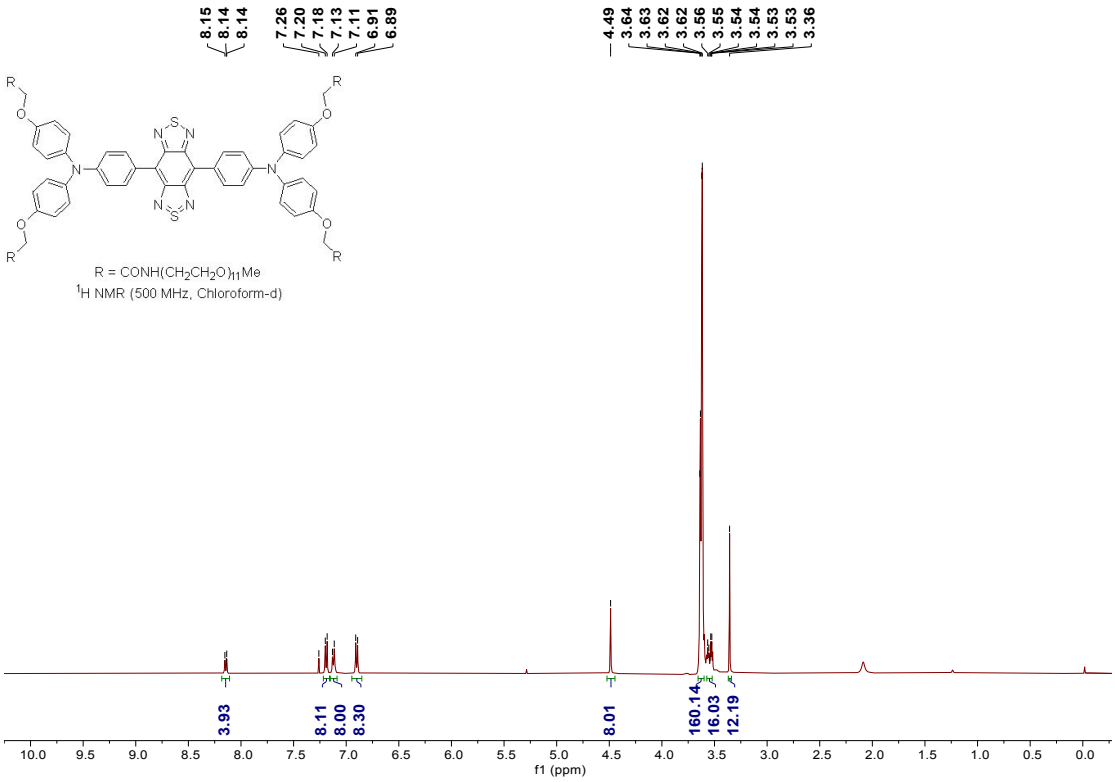

^{13}C NMR spectra of compound **BBT-OEG**

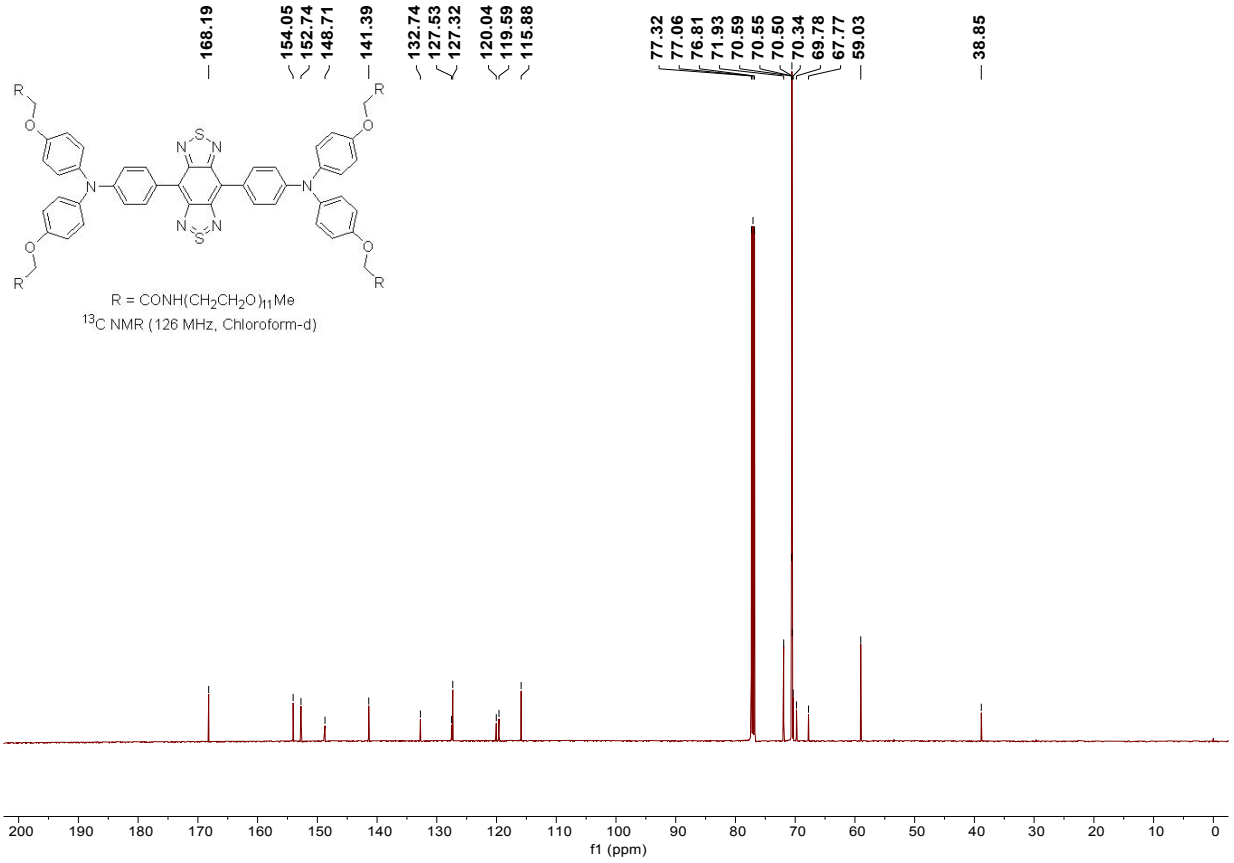

MALDI-TOF MS of compound **BBT-OEG**

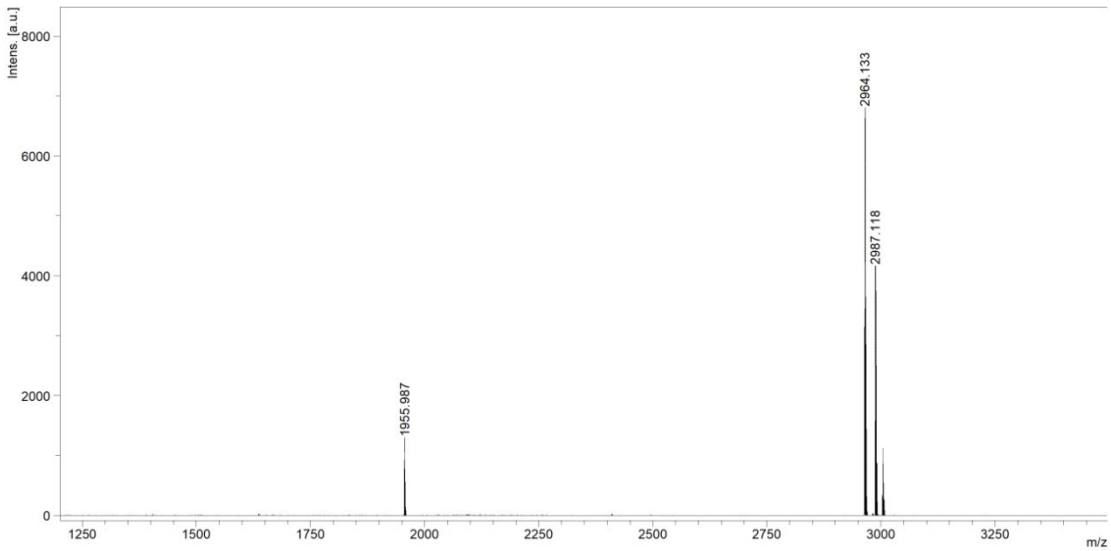

^{1}H NMR spectra of compound **BBT-C6**

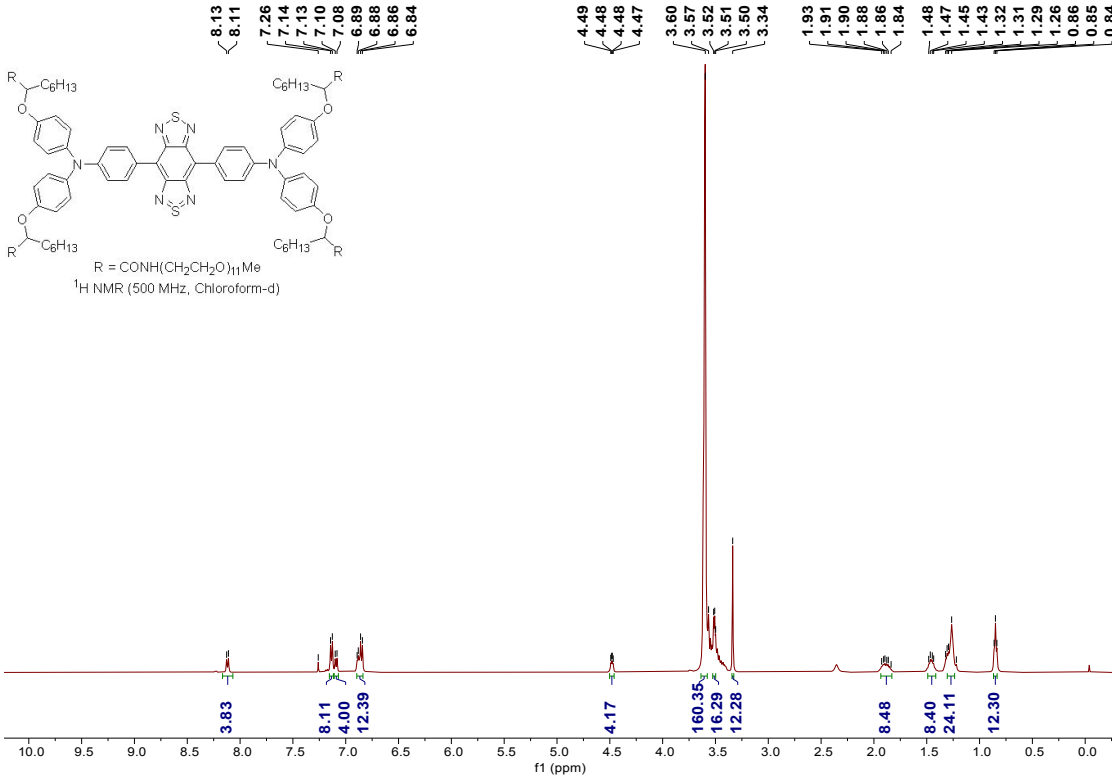

^{13}C NMR spectra of compound **BBT-C6**

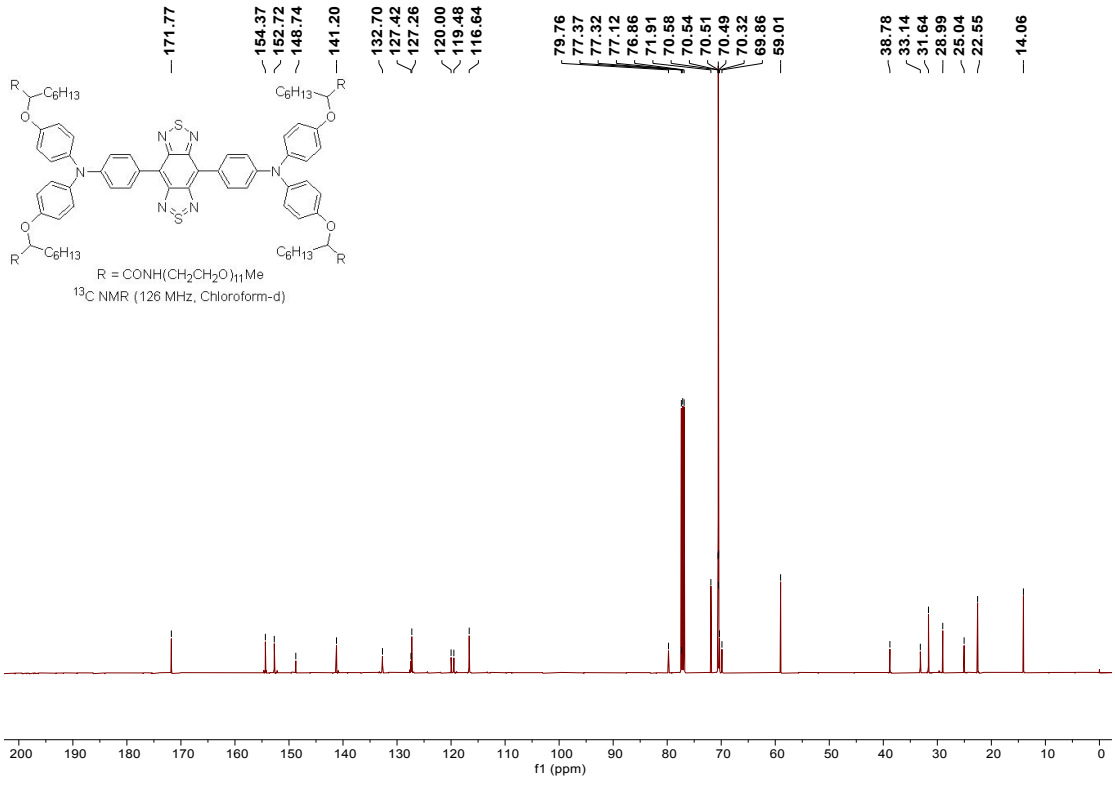

MALDI-TOF MS of compound **BBT-C6**

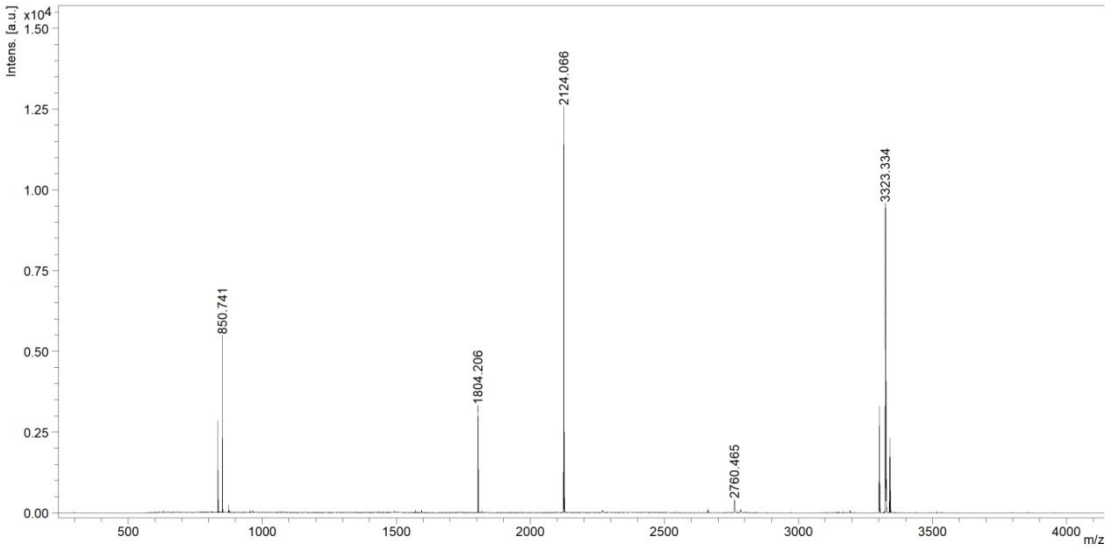

^{1}H NMR spectra of compound **BBT-C12**

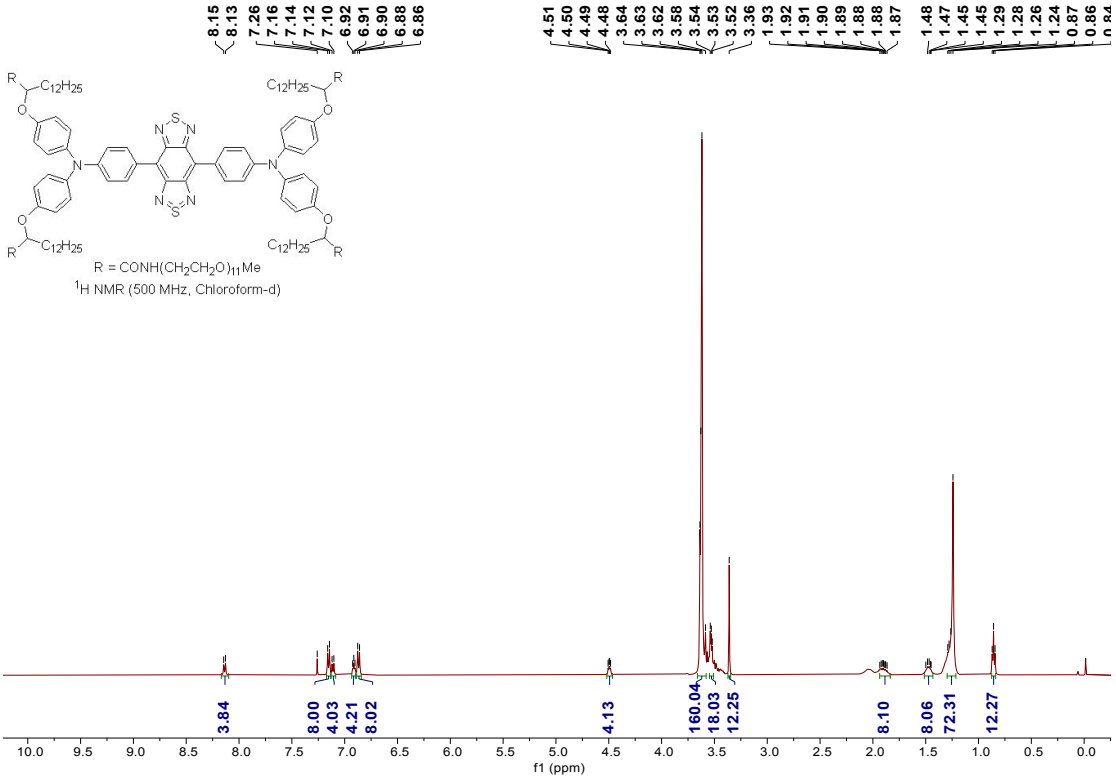

^{13}C NMR spectra of compound **BBT-12**

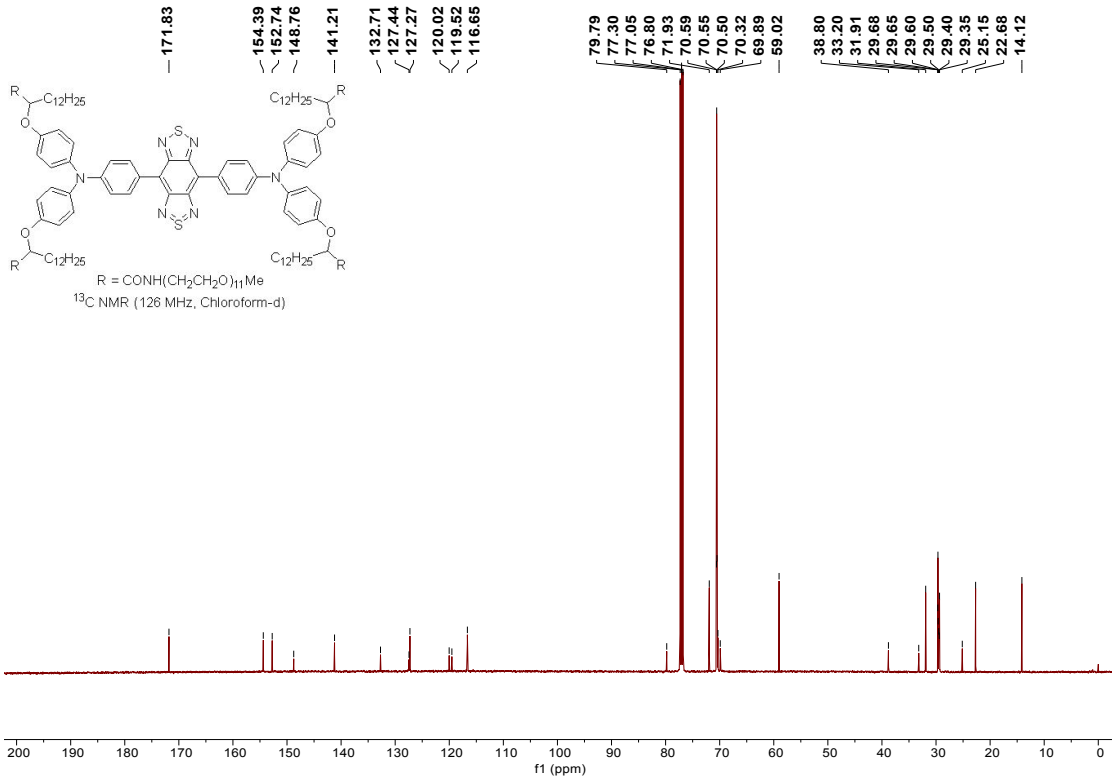

MALDI-TOF MS of compound **BBT-C12**

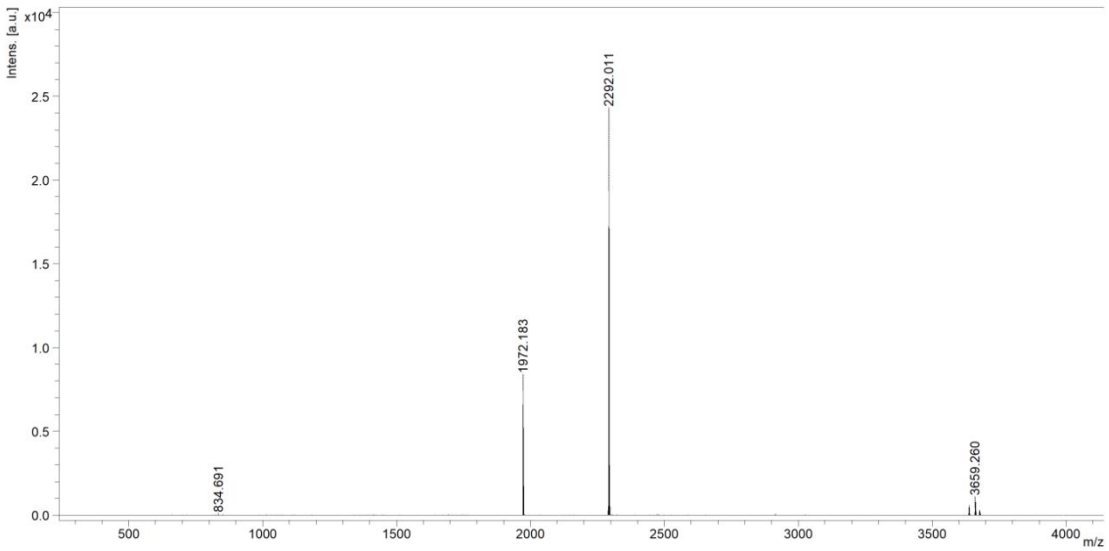

References

[1] S. Gao, G. Wei, S. Zhang, B. Zheng, J. Xu, G. Chen, M. Li, S. Song, W. Fu, Z. Xiao, *Nat. Commun.* **2019**, *10*, 2206.

[2] R. Zhang, Z. Wang, L. Xu, Y. Xu, Y. Lin, Y. Zhang, Y. Sun, G. Yang, *Anal. Chem*. **2019**, *91*, 12476-12483.

[3] G. Deng, X. Peng, Z. Sun, W. Zheng, J. Yu, L. Du, H. Chen, P. Gong, P. Zhang, L. Cai, B.Z. Tang, *ACS nano.* **2020**, *14*, 11452–11462.

[4] S. Yang, J. Zhang, Z. Zhang, R. Zhang, X. Ou, W. Xu, M. Kang, X. Li, D. Yan, R.T. Kwok, *J. Am. Chem. Soc.* **2023**, *145*, 22776-22787.

[5] S. Liu, X.Zhou, H.Zhang, H. Ou, J.W.Y. Lam, Y. Liu, L. Shi, D. Ding, B.Z. Tang, *J. Am. Chem. Soc.* **2019**, *141*, 5359–5368.

[6] Y. Xu, Y. Zhang, J. Li, J. An, C. Li, S. Bai, A. Sharma, G. Deng, J.S. Kim, Y. Sun, *Biomaterials* **2020**, *259*, 120315.

[7] R. Zhang, Y. Xu, Y. Zhang, H.S. Kim, A. Sharma, J. Gao, G. Yang, J.S. Kim, Y. Sun, *Chem Sci.* **2019**, *10*, 8348–8353.

[8] Y. Wang, W. Zhang, P. Sun, Y. Cai, W. Xu, Q. Fan, Q. Hu, W. Han, *Theranostics* **2019**, *9*, 391.

[9] S. Chen, B. Sun, H. Miao, G. Wang, P. Sun, J. Li, W. Wang, Q. Fan, W. Huang, *ACS Materials Lett.* **2020**, *2*, 174-183.

[10] X. Zeng, Y. Xiao, J. Lin, S. Li, H. Zhou, J. Nong, G. Xu, H. Wang, F. Xu, J. Wu, Z. Deng, X. Hong, *Adv. Healthc. Mater.* **2018**, *7*, e1800589.

[11] Y. Jiang, J. Li, X. Zhen, C. Xie, K. Pu, *Adv. Mater.* **2018**, *30*, 1705980.

[12] C. Huang, T. Shi, J. Zhang, Y. Sun, T. Ma, W. Li, Y. Li, H. Qiu, S. Yin, *Dyes Pigm*. **2023**, *210*. 110932.

[13] J. Liu, X. Zhang, M. Fu, X. Wang, Y. Gao, X. Xu, T. Xiao, Q. Wang, Q. Fan, *Biomater. Sci*. **2023**, *11*, 7124-7131.

[14] T. Li, C. Li, Z. Ruan, P. Xu, X. Yang, P. Yuan, Q. Wang, L. Yan, *Acs Nano* **2019**, *13*, 3691-3702.

[15] T. Sun, J. Han, S. Liu, X. Wang, Z.Y. Wang, Z. Xie, *ACS nano.* **2019**, *13*, 7345–7354.

[16] Y. Zheng, Y. Li, C. Ke, M. Duan, L. Zhu, X. Zhou, M. Yang, Z-X. Jiang, S. Chen, *J. Mater. Chem. B*, **2024**, *12*, 2373-2383.

[17] L.-G. r. Danielsson, Y.-H Zhang. *TrAC Trends Anal. Chem.* **1996**, *15*, 188-196.

[18] C. Yang, Y. Zhang, L. Sun, J. Wang, Z. Zhao, Z. Huang, W. Mao, R. Xue, R. Chen, J. Luo, T. Wang, J. Jiang, Y. Qin, *Adv. Funct. Mater.* **2022**, *33*, 2211251.

[19] C. Lehmann, T. Friess, F. Birzele, A. Kiialainen, M. Dangl, *J. Hematol. Oncol*. **2016**, *9*, 50.